Monthly Notices
of the
ROYAL ASTRONOMICAL SOCIETY

MNRAS **429,** 1652–1673 (2013) doi:10.1093/mnras/sts453

The *XMM*–Large Scale Structure catalogue – II. X-ray sources and associated multiwavelength data

L. Chiappetti,[1]★ N. Clerc,[2]† F. Pacaud,[3] M. Pierre,[2] A. Guéguen,[2]‡ L. Paioro,[1] M. Polletta,[1] O. Melnyk,[4,5] A. Elyiv,[4,6] J. Surdej[4] and L. Faccioli[2]

[1]*INAF, IASF Milano, via Bassini 15, I-20133 Milano, Italy*
[2]*Laboratoire AIM, CEA/ DSM/Irfu/SAp, CEA-Saclay, F-91191 Gif-sur-Yvette Cedex, France*
[3]*Argelander Institut für Astronomie, Universität Bonn, Auf dem Hügel 71, D-53121 Bonn, Germany*
[4]*Institut d'Astrophysique et de Géophysique, Université de Liège, Allée du 6 Août, 17, B5C, 4000 Sart Tilman, Belgium*
[5]*Astronomical Observatory, Kyiv National University, vul. Observatorna 3, 04053 Kyiv, Ukraine*
[6]*Main Astronomical Observatory, Academy of Sciences of Ukraine, vul. Akademika Zabolotnoho 27, 03680 Kyiv, Ukraine*

Accepted 2012 November 19. Received 2012 November 19; in original form 2012 June 22

ABSTRACT

We present the final release of the multiwavelength *XMM*–Large Scale Structure (LSS) data set, covering the full survey area of 11.1 deg^2, with X-ray data processed with the latest *XMM*–LSS pipeline version. The present publication supersedes the catalogue from the first paper in this series, pertaining to the initial 5 deg^2. We provide X-ray source lists in the customary energy bands (0.5–2 and 2–10 keV) for a total of 6721 objects in the deep full-exposure catalogue and 5572 in the catalogue limited to 10 ks, above a detection likelihood of 15 in at least one band. We also provide a multiwavelength catalogue, cross-correlating our list with infrared, near-infrared, optical and ultraviolet catalogues. Customary data products, such as X-ray FITS images and thumbnail images from the Canada–France–Hawaii Telescope Legacy Survey and the *Spitzer* Wide-Area Infrared Extragalactic Survey, are made available, together with our data base in Milan, which can be queried interactively. Also, a static snapshot of the catalogues has been supplied to the Centre de Données astronomiques de Strasbourg (CDS).

Key words: catalogues – surveys – X-rays: general.

1 INTRODUCTION

The rationale for the *XMM*–Large Scale Structure (*XMM*–LSS) survey was presented in Pierre et al. (2004), and a first catalogue for the 5.5 deg^2 survey, up to 2003, was presented in Pierre et al. (2007, hereafter Paper I). In the present paper, we supersede the first release with a new version, which covers the entire 11.1 deg^2 area of the survey. All of the data have been processed or reprocessed afresh with the latest version of our pipeline (see Section 3.1). We are releasing two families of X-ray data base tables (see Section 2.4), a standard catalogue (called `2XLSS`), for event files truncated to a common uniform exposure of 10 ks, and a deeper catalogue (called `2XLSSd`) using the full exposure time.

The *XMM*–LSS survey area, located around 2^h30^m -5°, has been covered: in the optical band, by the Canada–France–Hawaii Telescope Legacy Survey[1] Wide and Deep Synoptic fields (CFHTLS W1 and D1); in the near-infrared (NIR) band, partially by the United Kingdom Infrared Telescope (UKIRT) Infrared Deep Sky Survey[2] (UKIDSS; Lawrence et al. 2007); in the infrared (IR), by the *Spitzer* Wide-Area Infrared Extragalactic Survey[3] (SWIRE; Lonsdale et al. 2003); in the ultraviolet (UV), by the *Galaxy Evolution Explorer*[4] (*GALEX*; Martin et al. 2005) All-Sky Survey. We are also releasing a multiwavelength data base table (using data from the sources just described) in conjunction with each of the X-ray table families.

Data from the present catalogue have already been used in other works, published, submitted or in preparation (e.g. Adami et al. 2011; Elyiv et al. 2012; Clerc et al., in preparation; Melnyk et al. 2012; Willis et al. 2012).

The plan of the paper is as follows. In Section 2, we describe the layout and content of our catalogue. In particular, in Section 2.4, we present our data base system through which users can have public

★ E-mail: lucio@lambrate.inaf.it
†Present address: Max-Planck-Institut für extraterrestrische Physik, Giessenbachstraße, D-85748 Garching, Germany.
‡Present address: GEPI, Observatoire de Paris, CNRS, Université Paris Diderot, 5, place Jules Janssen, F-92195 Meudon, France.

[1] http://cfht.hawaii.edu/Science/CFHTLS/
[2] http://www.ukidss.org/
[3] http://swire.ipac.caltech.edu/swire/swire.html
[4] http://www.galex.caltech.edu/

access to all the data tables and associated data products. A reduced summary is available at the Centre de Données astronomiques de Strasbourg (CDS).[5] In Sections 3 and 4, we describe the X-ray data processing and the generation of the multiwavelength catalogue, respectively. Finally, we present some statistics in Section 5 and our concluding remarks in Section 6.

2 CATALOGUE LAYOUT AND CONTENT

2.1 List of available pointings

The entire *XMM*–LSS survey consists of 91 positions on the sky, arranged with a regular spacing. However, some of the pointings have been repeated once or twice, because the first observations were flagged as bad as a result of too high a background or insufficient clean exposure time. A total of 117 pointings were executed during the Guaranteed Time, AO-1, AO-2, AO-5 and AO-7 periods. In addition, from the archives, we have retrieved seven pointings of the independent Subaru *XMM–Newton* Deep Survey (SXDS; Ueda et al. 2008), with a different spacing but fully surrounded by our own pointings, and we have reanalysed these with our pipeline. The complete list of all 124 pointings is given in Table 1, while the layout on the sky is plotted in Fig. 1.

2.2 X-ray source lists

In this paper, we present two variants of the X-ray catalogue, each including source lists for two bands, 0.5–2 and 2–10 keV, called B and CD, respectively. The deep catalogue (`2XLSSd`) has been obtained from the processing of event files for the entire exposure of each pointing (with the exception of pointing S01, whose duration is much longer than all other pointings, and which has also been processed as a 'chunk' of 40 ks). The standard catalogue (`2XLSS`) instead uses a uniform exposure of 10 ks for all pointings longer than that. Both catalogues share an identical processing and the same layout. The list of data base columns are reported in Tables A1 and A2 in Appendix A.

2.3 Multiwavelength catalogues

We are also providing multiwavelength catalogues, in the data base called `2XLSSOPT` and `2XLSSOPTd` (see the list of data base columns in Table A3 in Appendix A), generated by correlating the X-ray source list with the optical, NIR, IR and UV catalogues described in Section 4.

2.4 Summary of online availability

2.4.1 Data base tables

The data base site at the Istituto di Astrofisica Spaziale e Fisica Cosmica (IASF) Milano, described in Paper I, has been relocated since 2007 August to the new site at http://cosmosdb.iasf-milano.inaf.it/XMM-LSS/. It has been converted to the DART interface (Paioro et al. 2008), which we have developed and used at the IASF to support several other projects. While the underlying MYSQL data base structure has been left virtually unchanged since the one described by Chiappetti et al. (2005), the user interface has been improved. In particular, it now requires public users to register with an individual username (see the instructions available from the home page).

In addition to the material described in Paper I (which will continue to remain available), the data base tables listed in Table 2 (plus the data products described in Section 2.4.2) are available in our data base, allowing fully interactive selection. Refer to Appendix A for the subset also available in electronic form at the CDS.

Single-band tables are provided separately for the B [0.5–2] keV and CD [2–10] keV bands. These contain a selection of parameters generated by XAMIN, such as both sets of values computed for the point-like and extended source fits. Position errors and fluxes are derived a posteriori, and computed as described in Section 3.1.1. Only sources above a detection likelihood of 15 are made available in the single-band tables. Redundant sources detected in overlapping regions of different pointings are removed, as explained in Section 3.4.

The B–CD band merged catalogue is obtained by matching single-band detections within a correlation radius of 10 arcsec (see Section 3.3), and includes only the parameters for the classification (point-like or extended) relative to the best band. Data in the other band are made available, even if they have a detection likelihood below 15.

2.4.2 Associated data products

Data products are files associated with a given data base entry. We distinguish the cases of per-pointing and per-object data products. When a data base query returns a number of X-ray sources, each of these could point to an individual data product, or to one common to the pointing where the source was detected. The data base interface allows the user to retrieve individual data products, or to build on the fly a `.tar.gz` file containing all the products related to the query.

2.4.2.1 X-ray images. The following X-ray data products are available per-pointing for the deep catalogue only.

(i) The B and CD band photon images (one mosaic cumulative for the three detectors, after the event filtering).
(ii) The B and CD wavelet images derived from the above.
(iii) Separate exposure maps for the three detectors and two bands.
(iv) The ds9 contours (log-spacing based on B-band wavelet images).

All images have a pixel size of 2.5 arcsec. Note that the World Coordinate System (WCS) of the X-ray images is the one generated by SAS, so it does not take into account the astrometric correction described in Section 3.2. Consequently, when overlaying X-ray source positions exactly on the X-ray images, it is necessary to use the coordinates labelled as 'raw' in Table A1, although this does not make much difference for most of the sources, given the pixel size.

2.4.2.2 Multiwavelength data. The following thumbnail images are available per X-ray source in association with the band merged and multiwavelength catalogues (deep version only). The FITS thumbnail images have a proper WCS, which allows direct overlaying of X-ray astrometrically corrected positions as well as counterpart positions.

(i) FITS CFHT images (40×40 arcsec^2) are available in the i' band for sources covered by the CFHTLS W1 or D1 fields and/or in the g' band when covered by our own ABC fields, obtained via the

[5] http://cdsweb.u-strasbg.fr

Table 1. The complete list of *XMM*–LSS pointings in chronological order of observation. Column 1 in each group of four is our own internal field name (the letter G refers to the Liège/Milan/Saclay Guaranteed Time, the letter B to Guest Observer time and the letter S to the SXDS; the suffixes a, b and c indicate repetition of a pointing because of insufficient exposure after high background filtering). Fields flagged as bad in column 3 have usually been repeated, except for B17c, B45b, B47b and B68b, which are the latest and best, though nominally bad, and are necessary in order to avoid holes in the covered area. Column 2 is the ESA ObsId identifier, which can be used to look up the pointing in the *XMM–Newton* log and archive. The exposure (in ks) indicated in column 4 is the weighted mean of MOS1, MOS2 and pn nominal exposures. These exposure times refer to `2XLSSd`. For `2XLSS`, all exposures longer than 10 ks have been curtailed to such a length at event file generation time.

(1)	(2)	(3)	(4)	(1)	(2)	(3)	(4)	(1)	(2)	(3)	(4)
S01	011237 0101	[a]	80.2[a]	B20	003798 2001		14.9	B49	040496 6301		10.5
S02	011237 0301		37.1	B21	003798 2101		12.6	B51	040496 6501		8.9
S03	011237 0401		15.7	B26	003798 2601		11.3	B52	040496 6601		12.5
S04	011237 1701		45.3	B27	003798 2701		13.8	B54	040496 6801		13.6
G17	011111 0301		20.6	B17a	003798 1701	bad	3.3	B55a	040496 6901	bad	6.6
G18	011111 0401		23.9	B18	003798 1801		13.7	B56	040496 7001		13.5
G13	010952 0501		21.4	B19	003798 1901		10.9	B57	040496 7101		10.5
G19	011111 0501		20.5	G03	011268 0301		20.7	B59	040496 7301		10.7
G15	011111 0101		16.9	B25	003798 2501		8.6	B60	040496 7401		13.5
G16a	011111 0201	bad	3.7	B24	003798 2401		14.0	B61a	040496 7501	bad	6.4
G16b	011111 0701		9.1	B23	003798 2301		7.9	B62	040496 7601		10.4
B01	003798 0101		11.6	B22a	003798 2201	bad	5.1	B63	040496 7701		12.6
B06	003798 0601		10.4	B28	014711 0101		10.4	B64	040496 7801		13.6
B02	003798 0201		10.5	B29	014711 0201		9.5	B65	040496 7901		13.5
B07	003798 0701		9.4	B30	014711 1301		11.4	B66	040496 8001		13.5
B03	003798 0301		10.7	B31	014711 1401		10.0	B67a	040496 8101	bad	4.8
B05	003798 0501		13.4	B32a	014711 1501	bad	1.6	B68a	040496 8201	bad	2.0
B04a	003798 0401	bad	5.9	B42a	040496 5601	bad	10.6	B69	040496 8301		8.7
B09	003798 0901		11.4	B58a	040496 7201	bad	6.0	B70a	040496 8401	bad	4.5
G01	011268 0101		24.2	B44a	040496 5801	bad	5.4	B72	040496 8601		11.8
G04	010952 0101		23.3	B53	040496 6701		9.4	B71	040496 8501		10.8
G10	010952 0201		22.0	B48	040496 6201		9.4	B58b	055391 1401		23.5
G07	011268 1001		22.2	B04b	040496 0101	bad	8.9	B61b	055391 1601		12.2
G09	010952 0601		19.5	B13b	040496 0201	bad	4.8	B70b	055391 1901		10.6
G14	011268 0801		11.0	B17b	040496 0301	bad	6.0	B44b	055391 0901		23.2
G12a	010952 0401	bad	1.7	B32b	040496 0401		10.5	B45b	055391 1001	bad	8.1
G11	010952 0301		19.3	G12b	040496 0501		9.5	B46b	055391 1101		21.1
G05	011268 0401		21.7	B22b	040496 0601		8.8	B04c	055391 0101		10.5
B08	003798 0801		8.7	B33	040496 4701		9.3	B13c	055391 0201		10.6
G02	011268 0201		8.9	B34	040496 4801		9.2	B17c	055391 0301	bad	7.8
B10	003798 1001		10.9	B35a	040496 4901	bad	5.1	B35b	055391 0401		10.0
B11	003798 1101		10.0	B36a	040496 5001	bad	8.1	B47b	055391 1201	bad	6.3
B12	003798 1201		9.4	B37a	040496 5101	bad	8.0	B36b	055391 0501		10.6
B13a	003798 1301	bad	4.4	B38	040496 5201		10.6	B50b	055391 1301		9.7
B14	003798 1401		9.3	B39	040496 5301		10.4	B41b	055391 0701		11.2
G08	011268 0501		19.0	B40	040496 5401		14.2	B42b	055391 0801		12.5
B15	003798 1501		10.3	B41a	040496 5501	bad	4.4	B37b	055391 0601		14.3
B16	003798 1601		10.2	B43	040496 5701		13.4	B55b	055391 1501		12.6
G06	011268 1301		13.4	B45a	040496 5901	bad	6.8	B67b	055391 1701		12.4
S06	011237 0701		46.9	B46a	040496 6001	bad	7.0	B68b	055391 1801	bad	4.9
S07	011237 0801		35.8	B47a	040496 6101	bad	5.9				
S05	011237 0601		32.7	B50a	040496 6401	bad	4.8				

[a]For field S01, the full exposure is much longer than the typical *XMM*–LSS exposure. For this reason, the relevant data are fictitiously flagged bad in `2XLSSd`, while those deriving from an analysis curtailed at 40 ks are used instead, with a field name of S01_40 in column 1 and an exposure of 40.0 ks in column 4.

Canadian Astronomy Data Centre (CADC) cutout service.[6] A PNG version is also available, as for Paper I.

(ii) FITS SWIRE images are available in the four IRAC bands (30×30 arcsec^2) and in the three bands for the Multiband Imaging Photometer for *Spitzer* (MIPS; 60×60 arcsec^2), obtained via the Infrared Processing and Analysis Center (IPAC) GATOR cutout service.[7]

[6] http://www.cadc-ccda.hia-iha.nrc-cnrc.gc.ca/
[7] http://irsa.ipac.caltech.edu

3 X-RAY DATA PROCESSING

The original XAMIN pipeline used in Paper I has been described in detail by Pacaud et al. (2006). Although we refer to such papers for detail, here we summarize the main processing steps.

Standard SAS tasks are used to generate event lists. They are filtered for solar soft proton flares and used to produce images for the three EPIC detectors, which are then co-added in each energy band. Such per-band images are filtered in wavelet space, and scanned by a source detection algorithm based on SEXTRACTOR (Bertin &

Table 2. Data base tables of the current release.

Data sets	Tables
10-ks catalogues	
Merged catalogue (all parameters)	`2XLSS`
Single-band catalogues	`2XLSSB, 2XLSSCD`
Multiwavelength catalogue	`2XLSSOPT`
Deep catalogues	
Merged catalogue (all parameters)	`2XLSSd`
Single-band catalogues	`2XLSSBd, 2XLSSCDd`
Multiwavelength catalogue	`2XLSSOPTd`
XMDS catalogues	
Multiband X-ray catalogue	`XMDS`
Multiwavelength catalogue	`XMDSOPT`

Arnouts 1996) to obtain a primary source list. Source characterization is then performed with XAMIN, a maximum likelihood profile fitting procedure, designed for the *XMM*–LSS survey, optimized for extended X-ray sources and associated signal-to-noise regimes. XAMIN performs parallel fits with two classes of surface-brightness models – point-like and extended (β-profile) – and outputs the main parameter for both models in a FITS table per pointing and per band. Further processing (as described in Sections 3.2, 3.3 and 3.4) is performed contextually or after ingestion of XAMIN output into our data base.

3.1 Revised pipeline

For this release, we have used the latest version *pro tempore* (3.2) of XAMIN, which has been improved while translating it from IDL to PYTHON (open source). All pointings, including those reported in the `XLSS` catalogue in Paper I, have been (re)processed afresh with this latest version.

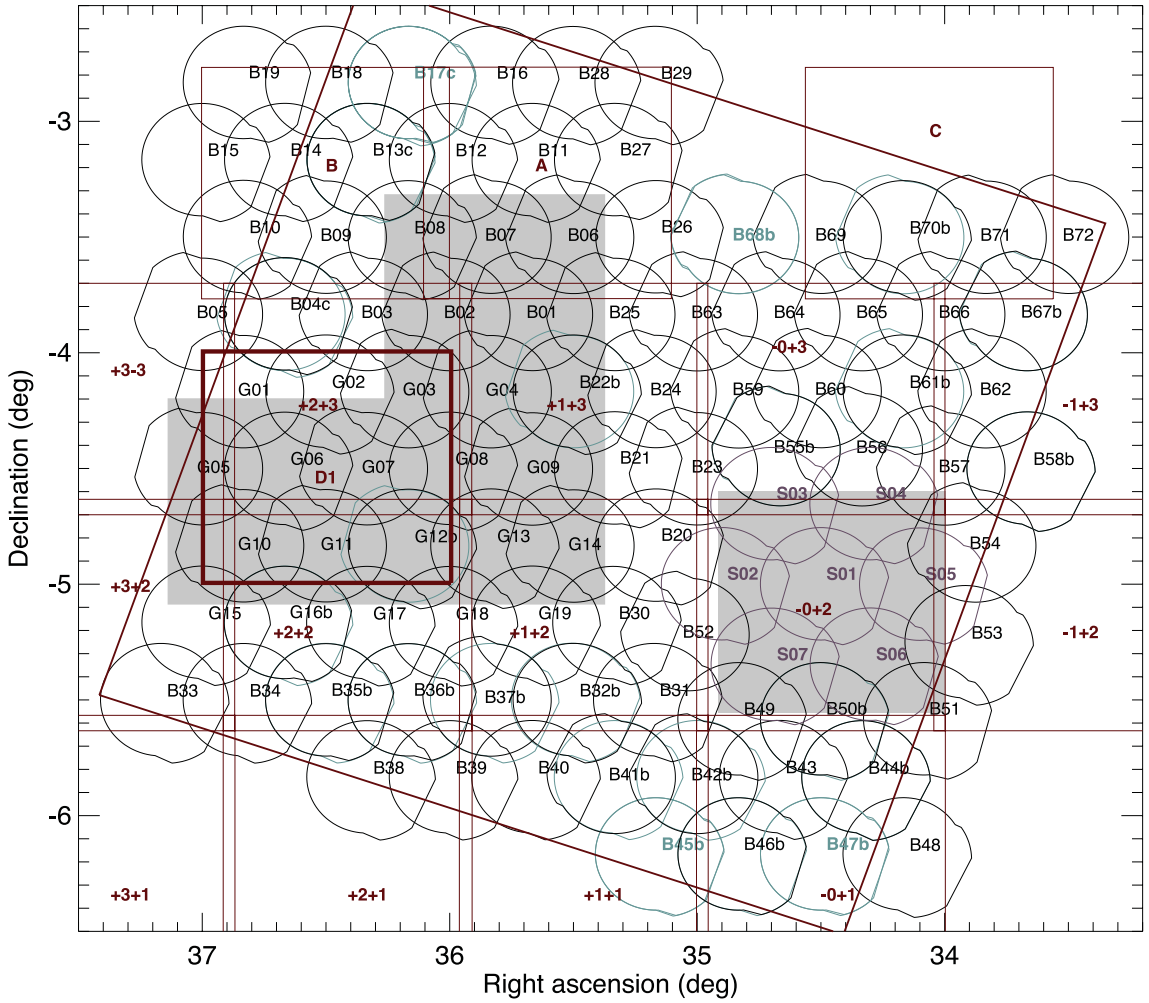

Figure 1. Layout of the *XMM*–LSS pointings and coverage in other wavebands. The positions of the footprints of good pointings in the *XMM* field of view are plotted and labelled with their field name (in black). SXDS pointings are plotted and labelled in grey (pink-grey in the online version). Bad pointings (later repeated by good pointings) are plotted in light grey (blue-grey in the online version), without labels (except for the four cases where even the last re-observation is nominally bad). The total geometrical area is estimated to be 11.1 deg^2. The dark grey (maroon in the online version) squares indicate the various tiles of the CFHTLS W1 survey (labelled with their short $\pm x \pm y$ name; see http://terapix.iap.fr/cplt/oldSite/Descart/cfhtls/cfhtlswidemosaictargetW1.html), of our own supplementary pointings (labelled ABC) and the CFHTLS D1 field (thick). The large tilted square is the area covered by the SWIRE survey. The shaded areas are those covered by the UKIDSS surveys (DXS, left; UDS, right) in release DR5plus. The entire area is covered by the *GALEX* All-Sky Imaging and Deep Imaging Surveys.

The XAMIN pipeline output parameters for version 3.2 are the same listed in table 2 of Paper I (and flagged in column X in Tables A1 and A2).

The event file generation (and the subsequent pipeline) was applied independently to the full exposure of each pointing, as well as to 10-ks curtailed chunks (from the beginning of the exposure). The latest *XMM* calibrations available *pro tempore* have been applied.

One of the differences between the old and new pipelines is the correction of an offset of 0.5 pixel (where our pixel size is 2.5 arcsec) in the *XY* image positions. For this reason, all X-ray source positions and catalogue names (see Section 3.5) have changed.

We have checked that the new pipeline version provides results consistent with the previous IDL version by performing detailed tests on simulated and real *XMM* pointings. Then, we have proceeded to a direct comparison, which shows a (good) agreement between the old and new pipelines, as reported in Appendix C1.

The following is a summary list of all differences in catalogue generation with respect to Paper I:

(i) more input data (5–11 deg^2);
(ii) used latest SAS version and calibrations;
(iii) used XAMIN version 3.2;
(iv) in particular, half-pixel offset cured (see above);
(v) astrometry using CFHTLS T004 (see Section 3.2);
(vi) band merging at 10 arcsec (see Section 3.3);
(vii) overlap removal at 10 arcsec (see Section 3.4);
(vii) web site relocated (see Section 2.4);
(ix) more multi-λ bands (see Section 4).

In addition to the XAMIN output, a number of parameters are calculated a posteriori in order to facilitate the interpretation of the data set. Because, in its present state, XAMIN does not perform error calculations, mean statistical errors were estimated by means of extensive simulations, as explained in Paper I and Pacaud et al. (2006). We note that only the first two digits are to be considered significant for the count rate and for the core radius as well as for the derived quantities.

Analogously to Paper I, only sources with an off-axis angle <13 arcmin are processed by XAMIN. The catalogues include all the extended sources classified in the customary C1 and C2 classes (see Section 3.6) plus all point-like sources with a point source detection likelihood (*LH*) greater than 15 (so-called non-spurious sources). The resulting sky coverage is shown in Fig. 2.

3.1.1 *Count rate and flux*

As in Paper I, fluxes are not computed by XAMIN but are inserted in the catalogue as derived parameters. That is, a single mean flux ([FLUX(MOS)+FLUX(pn)]/2) is computed from the count rates using the customary conversion factors reported in Table 3, assuming the spectral model given in its caption.

The observed log N–log S distributions are presented in Fig. 3, reproduced in a simplified form from Elyiv et al. (2012).

Photometric accuracy plots based on simulations were presented in fig. 3 of Paper I as a function of different off-axis angle ranges. Further simulations were performed considering different background levels as an additional parameter. These are presented, supplementing Paper I, in Fig. 4. Note that the background factors of 0.25, 1 and 4 refer to the nominal particle backgrounds defined in table 1 of Elyiv et al. (2012); we refer to this paper for details, and it also gives an alternative view in its figs 11 and 12. We conclude that the extremely weak dependency on background (if any) does not require us to introduce it into the parametrization of photometric bias and accuracy as a function of count rate and off-axis angle published in table 6 of Paper I.

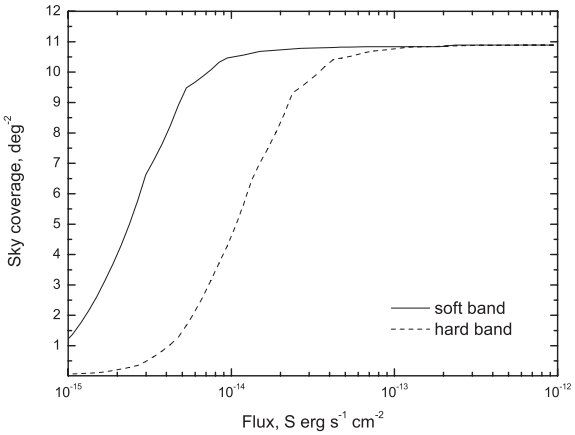

Figure 2. Effective sky coverage for the entire *XMM*–LSS area in the soft (B, [0.5–2] keV) and hard (CD, [2–10] keV) bands. This figure, reproduced from fig. 9 of Elyiv et al. (2012), updates and supersedes fig. 2 of Paper I. The computation derives from simulations of realistic *XMM*–LSS observations processed by XAMIN.

Table 3. The energy conversion factors for the individual EPIC cameras and energy bands, in units of 10^{-12} erg s^{-1} cm^{-2} for a rate of one count s^{-1}. A photon-index power law of 1.7 and a mean $N_{\rm H}$ value of 2.6×10^{20} cm^{-2} are assumed. The two MOS cameras are assumed to be identical.

Detector	B band	CD band
MOS	5.0	23
pn	1.5	7.9

3.2 Positional accuracy and astrometric corrections

The XAMIN pipeline does not directly provide error values, because, for efficiency purposes, the likelihood surface is only searched for its maximum. Therefore, identically to what was done in Paper I, the positional (statistical) error on the (point-source) coordinates is estimated from Monte Carlo simulations, and the values indicated in the catalogue are computed from a look-up table of discrete values as a function of count rate and off-axis angle ranges (as reported in Table 4). The distribution of the errors is shown in Fig. 5(b).

Similarly to Paper I, in order to compensate for possible systematic inaccuracies in the *XMM* pointing positions, a global rigid astrometric correction was estimated using the SAS task EPOSCORR (with rotational offset search disabled). The correction offsets were computed afresh for the full exposure case, and applied to both the `2XLSSd` and `2XLSS` catalogues.

For each pointing, the input to EPOSCORR was an X-ray reference file with all non-spurious X-ray sources, while optical reference files were generated by taking all objects in the CFHTLS W1 fields within 6 arcsec from the (raw) source position, brighter than $i' = 25$ (or $r' = 25$ for the ABC fields; see Section 4.1), and having a chance probability (as defined in Section 4.3) $prob < 0.03$. In case there were more possible counterparts, the one with the smallest probability was taken. Fields B68a and B68b (both bad) had no

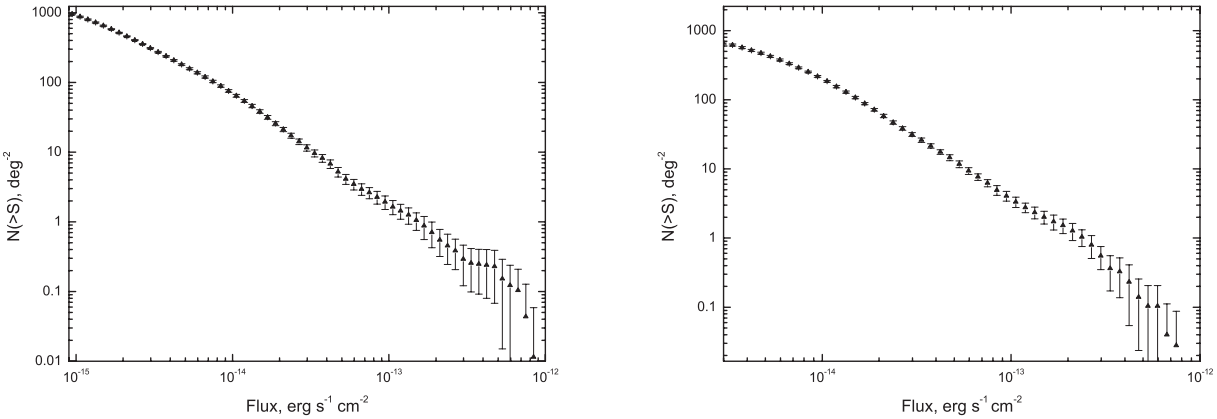

Figure 3. The log N–log S distributions for the soft (left-hand panel) and hard (right-hand panel) bands for the entire *XMM*–LSS area. These figures are reproduced in a simplified form from figs 13 and 14 of Elyiv et al. (2012).

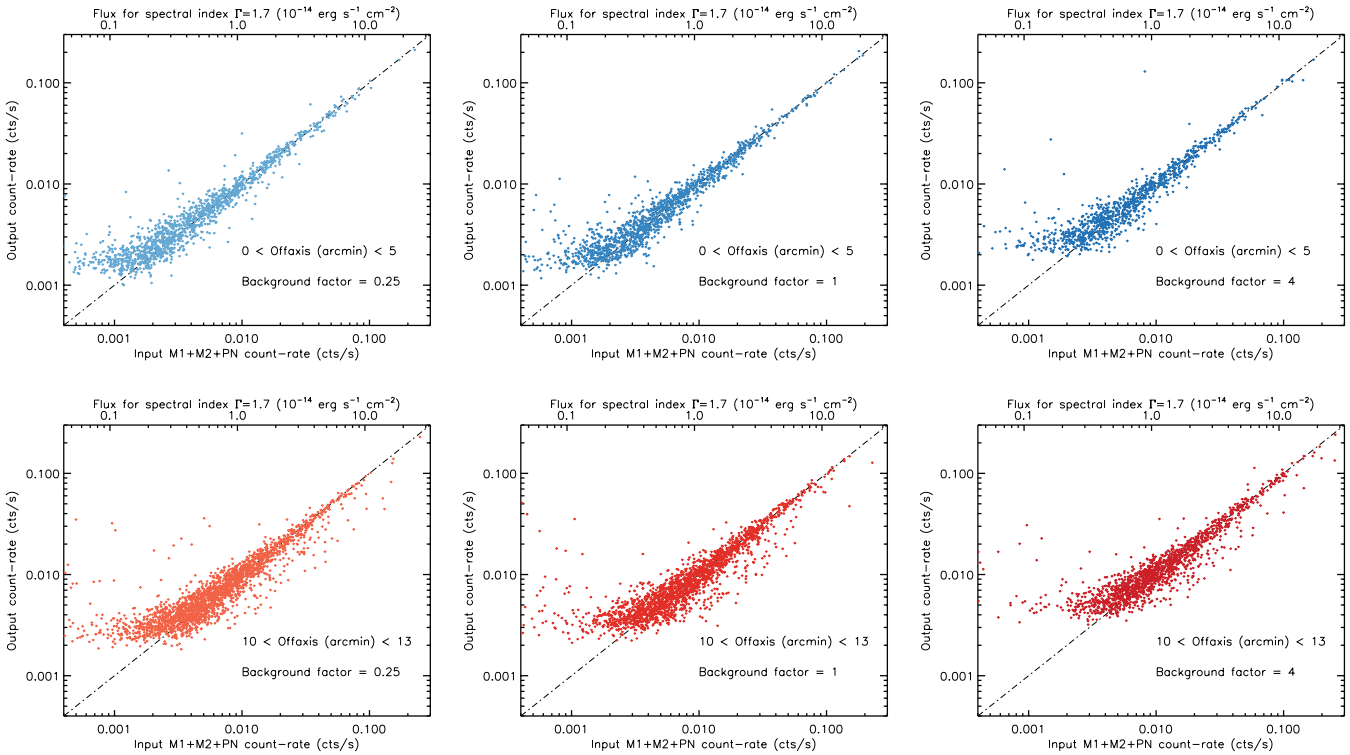

Figure 4. Photometric accuracy for three background values (see text) and two off-axis angle ranges (top, 0–5 arcmin; bottom, 10–13 arcmin; the plots for the intermediate range are similar). The count rate is the measured MOS1+MOS2+pn rate, normalized to the on-axis value.

CFHT counterparts and were corrected using stars in USNO A2.0. Field G12a (bad) had no counterparts at all and was not corrected.

The offsets computed by EPOSCORR were applied to all coordinate sets for each source in the data base. Astrometrically corrected positions were used in the subsequent operations: removal of the redundant sources, source naming and cross-identification with the catalogues in other wavebands.

In most cases, the offsets are small and barely significant.[8] The range of the RA offset is $-3.7 < \Delta\mathrm{RA} < 1.1$ arcsec (with just 16 pointings with $|\Delta RA| > 2$ arcsec, 27 pointings with a significance of the offset greater than 3σ, of which 13 were above 4σ). The range of the declination offset is $-2.7 < \Delta\mathrm{Dec.} < 2.7$ arcsec (with just four pointings with $|\Delta\mathrm{Dec.}| > 2$ arcsec, seven pointings with a significance greater than 3σ, of which three were above 4σ).

The quality of the positional accuracy can be estimated a posteriori from figures such as Figs 5 and 8. For the final statistics, see Section 5.2.

3.3 Band merging

The XAMIN pipeline has been optimized for the detection of clusters (which occurs preferentially in the soft band), and its wavelet filtering component is inherently working on a single band (see Pacaud et al. 2006, and references therein). Therefore, it is natural that energy bands are treated separately and the merging is performed at

[8] Tabulated online at http://cosmos.iasf-milano.inaf.it/I~ssadmin/Website/LSS/List/.newastroreport.html.

Table 4. Positional accuracy (1σ error on RA or Dec.) for point sources derived from simulations of 10-ks pointings and having a detection likelihood >15. Values are given for the B and CD bands, as a function of the summed measured count rate: CR = MOS1+MOS2+pn. This table is reproduced from table 8 of Paper I, to which the reader is referred for further details.

Count rate (count s^{-1})	B band Error (arcsec)	CD band Error (arcsec)
0 < off-axis < 5 arcmin		
0.001 < CR < 0.002	2.0	2.0
0.002 < CR < 0.005	1.7	1.7
0.005 < CR < 0.01	1.3	1.3
CR > 0.01	0.8	0.8
5 < off-axis < 10 arcmin		
0.001 < CR < 0.002	2.0	2.0
0.002 < CR < 0.005	1.8	1.9
0.005 < CR < 0.01	1.5	1.5
CR > 0.01	1.0	1.0
10 < off-axis < 13 arcmin		
0.001 < CR < 0.002	–	–
0.002 < CR < 0.005	1.9	2.0
0.005 < CR < 0.01	1.6	1.7
CR > 0.01	1.2	1.3

the post-processing stage, namely in the data base ingestion stage. As in Paper I, we intend to provide an X-ray band-merged catalogue along with the single-band catalogues. Such a merging procedure was defined in Paper I to cope with the case that an X-ray source can be detected in one or two bands and, for each band, can be independently fitted by the extended and point-source models with the coordinates free. For each band, a source is classified as extended (E), as described in Section 3.6; otherwise, it is classified as point-like (P). Then, pointing by pointing, we flag associations between the two bands within a search radius of 10 arcsec. Note that we allow associations involving spurious sources (LH < 15) at most in one band. We keep the information (rate, flux, etc.) about entries below this threshold in the merged catalogue, because it could be more useful (e.g. for upper limits) than no information at all, but we flag those cases with `Bspurious` = 1 or `CDspurious` = 1. Finally, for each soft–hard couple in the merged catalogue, we define the best band (i.e. the band in which the detection likelihood of the source is the highest and from which the coordinates are taken). The source flagging and classification (and the way fluxes appear in the data base) is identical to the one described in table 9 of Paper I.

What has changed from Paper I is the search radius, which has increased from 6 to 10 arcsec. In fact, an examination of the `XLSS` catalogue shows an excess of couples of soft-only and hard-only sources usually detected in the same pointing with a distance marginally above 6 arcsec. Either these could be interpreted as potential missed mergers, because they might have escaped band merging as a result of the distance, or, if they were in different pointings, they could be potential missed overlaps. We have performed a thorough analysis of sources closer than 30 arcsec. We have found that 95 per cent of the detections in the same field before band merging, closer than 10 arcsec, meet the definition of missed mergers, while only 25 per cent of those farther than 10 arcsec do.

The starting point is represented by the individual band tables. After the initial merging procedure for `2XLSSd`, it is possible to directly compare the 10- and 6-arcsec merging, as shown in Table 5. Here, preserved means they are either unmerged (single-band

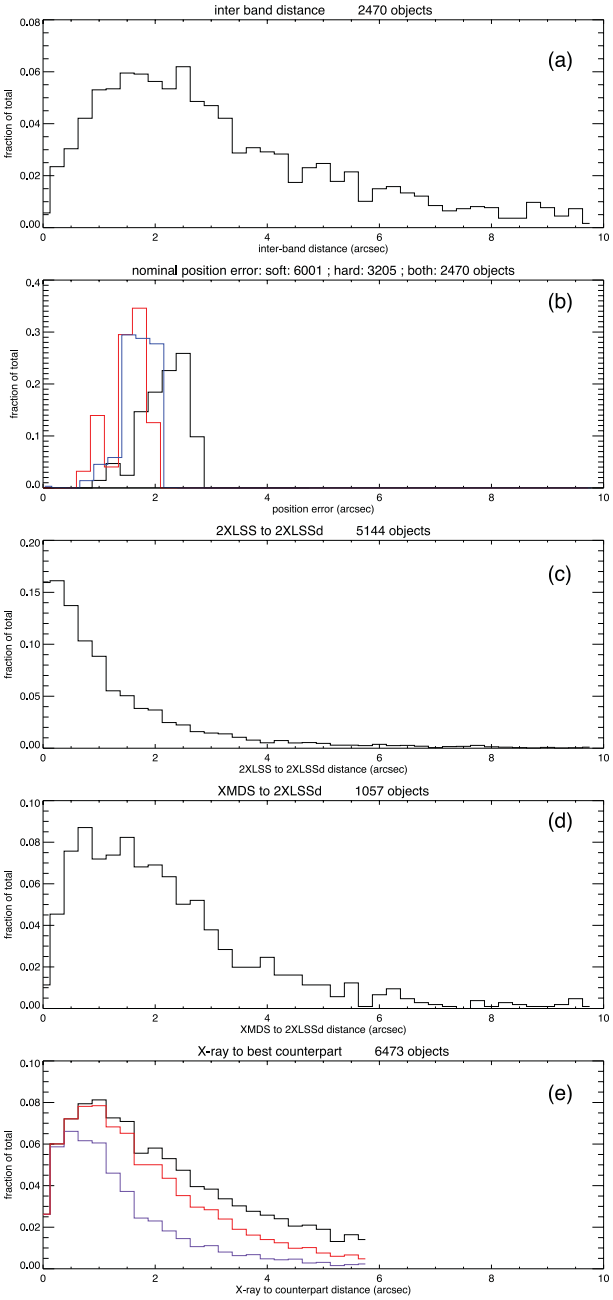

Figure 5. Histograms (as a fraction of the total number of objects indicated in each panel title) of distances or positional parameters for the `2XLSSd` catalogue. (a) The distribution of the interband distance `Xmaxdist` for objects detected in both energy bands. (b) The distribution of the position errors for the soft (light-grey histogram; red in the online version) and hard (light-grey histogram; blue in the online version) bands, and of their combined errors for sources detected in both bands (black histogram). (c) The distance between the X-ray positions in the two catalogues for objects common to `2XLSSd` and `2XLSS` (both resulting from same XAMIN pipeline). (d) The distance between the X-ray positions in the two catalogues for objects common to `2XLSSd` and XMDS (different event file reduction and different pipeline; see Appendix C3). (e) The distribution of the distance between the X-ray position and the position of the best counterpart in the optical, NIR, IR or UV bands. The black histogram is for all objects with a counterpart (of any quality) in at least one non-X-ray band. We also show (as a fraction of the same total) the distributions for the counterparts having either good or fair probability (light-grey histogram; red in the online version), and for those having good probability (grey histogram; violet in the online version).

Table 5. Statistics of the band-merging procedure.

Number of sources for condition	Total	Non-spurious
In input soft-band table	10 348	7339
In input hard-band table	7124	3235
After initial merging	14 216	
Of which preserved w.r.t. 6-arcsec merging	13 713	7824
Of which upgraded	505	457
Lost (no longer considered)	492	
`Xmaxdist` $<$ 2 arcsec	33 per cent	37 per cent
`Xmaxdist` $<$ 4 arcsec	69 per cent	75 per cent
After 'divorce' procedure		
Preserved	13724	
Upgraded	492	

detection) or merged in the same way, and identical in all respects. Upgraded means they would have been considered at 6 arcsec as detections in a single band, and are merged into one at 10 arcsec. Lost means single-band detections at 6 arcsec which are no longer considered.

As already described in Paper I, there are a limited number of cases where the band merging is primarily ambiguous, and a source in a band happens to be associated with two different objects in the other band (i.e. it gives rise to a couple of entries in the merged table). The implication on source naming is discussed in Section 3.5. In a further step of the band-merging procedure, we have also considered secondary ambiguous cases based on the interband distance (data base column `Xmaxdist`) between the positions found by XAMIN in the two energy bands. If in a couple both `Xmaxdist` < 6 arcsec (i.e. they would also have been ambiguous with the old merging) or both `Xmaxdist` > 6 arcsec (i.e. irremediably ambiguous), both merged entries are maintained; when one `Xmaxdist` is below 6 arcsec and the other above, the latter entry is divorced. The lower-distance element remains a merged two-band detection, while the other is reset to a hard-only or soft-only source.

Note that not all sources in the produced merged table will go into the catalogue: those that are spurious in both bands will not be included, as well as those removed as redundant according to the procedure in Section 3.4. The total number of ambiguous cases in the final catalogue is small: 20 couples and five singles (over 6721) for `2XLSSd` and 15 couples and eight singles (over 5572) for `2XLSS`.

For sources detected in both energy bands, the interband distance `Xmaxdist` is an additional indicator, besides the nominal position error described in Section 3.2. Its distribution is reported in Fig. 5(a). If we compute a statistical position error σ combining quadratically the nominal errors in the two bands, we can also see that for `2XLSSd` 38 per cent have `Xmaxdist` $\leq \sigma$, 76 per cent within 2σ and 93 per cent within 3σ (for `2XLSS`, the percentages are 30, 67 and 88 per cent, respectively).

3.4 Removal of redundant sources

As in Paper I, in the case of redundant objects detected in the regions where the pointings overlap, we keep in the catalogue only the detection pertaining to the pointing where the source is the closest to the optical centre (columns `Boffaxis`, `CDoffaxis` in the data base). Because overlap removal is the final stage of catalogue building, it is here that sources with $LH < 15$ are discarded and only non-spurious sources are brought forward. However, at variance with Paper I, for analogy with the band merging, redundant objects are associated within a larger radius of 10 arcsec. Moreover, the off-axis angle criterion is applied only if the overlapping pointings are both flagged good or both bad; otherwise, the source in the good pointing prevails unconditionally.

The overlap removal affects 1574 entries in `2XLSSd` and 1205 in `2XLSS`.

Note that the present catalogue also contains a few sources in fields flagged bad. An extremely conservative usage might exclude all sources detected in bad fields using condition `Xbadfield` $= 0$. A less conservative usage should include the four (bad, non-reobserved) fields mentioned in the caption of Table 1.

3.5 Source naming

Application of the latest XAMIN version, of the updated CHFTLS T004 astrometric corrections and of the 10-arcsec radius in the band merging and overlap removal stages, implies that, even in the pointings already covered by the Version I `XLSS` catalogue, a source might be sometimes superseded by a different choice, and might have slightly different coordinates. The same applies to the two processings (full exposures and 10-ks exposures). Combined with the IAU requirement that once a source in a catalogue has been assigned a name (even if this is a coordinate name), the name cannot change even if the actual coordinates are improved (modified), unless a completely new catalogue is issued, this leads us to define the following naming convention.

(i) The official catalogue name `Xcatname` is now generated in the form `2XLSS Jhhmmss.s-ddmmss`, or respectively `2XLSSd Jhhmmss.s-ddmmss`, where, as in Paper I, the coordinates used in assigning the name are the ones deduced after the rigid astrometric correction, and chosen as official (i.e. those for the best band; see Table A2).

(ii) The single-band catalogue names `Bcatname` and `CDcatname` use the unofficial prefixes `2XLSSB` or `2XLSSCD` for both the deep and 10-ks catalogues. However, as in Paper I, the coordinates used in the name correspond to the extended (E) or point-like (P) fit in the relevant band (Table A2).

(iii) The reference to the `XLSS` source replaced by a `2XLSS` or `2XLSSd` source is possible using column `Xlsspointer`, which contains the value of `Xseq` in the table `XLSS` (an explicit look-up in the latter table is necessary to find its name or other characteristics).

(iv) Similarly, when accessing `2XLSS`, it is possible to use column `Xdeep`, which points to the value of the `Xseq` closest source in `2XLSSd`.

As described in Section 3.3, in a small number of cases, a source in a band happens to be associated with two different objects in the other band. These couples of catalogue entries are flagged by a non-zero value in column `Xlink`. Consistently with the convention defined in Paper I, the ambiguity in the name is resolved (when necessary; i.e. in one case for `2XLSSd` and in three cases for `2XLSS`) by the addition of a suffix (e.g. the two members of a couple will appear as `2XLSS JHHMMSS.S-DDMMSSa` and `2XLSS JHHMMSS.S-DDMMSSb`).

3.6 Extended source classification

The extended source classification is the same as described in Paper I. Extended sources are selected from the XAMIN parameter space as detections with `extent` >5 arcsec and `likelihood of extent` $>$ 15. They are further divided into two classes: C1 with `likelihood of extent` > 33 and `likelihood of detection` > 32, which is almost uncontaminated by misclassified point sources, and C2

Table 6. Statistics of extended sources.

Classification and catalogue	2XLSS	2XLSSd
Sources with Bc1c2 $\neq 0$	147	160
of which C1	49	53
of which C2	98	107
Total number of extended sources	187	210
of which C1	54	57
of which C2	133	153
extended in both bands	4	4
soft C1 detected in both bands	9	12
soft C2 detected in both bands	12	16
soft only C1	36	37
soft only C2	86	91
hard only C1	5	4
hard only C2	35	46

(the rest), allowing for ≈50 per cent contamination. This classification is stable even in the case of changes in the exposure time or background, as shown in fig. 9 of Clerc et al. (2012)

The catalogues report only the flagging as an extended source in the soft band (column Bc1c2). However, for the unique purpose of band merging, the same classification has nominally been applied also to the hard band. A short statistics is reported in Table 6, while the compatibility in the two catalogues (compatible means extended in both catalogues in the (prevailing) band where it is detected, and undetected (or point-like) in the other band) is shown by the following breakdown:

95 sources with the same extended classification;
eight sources with a compatible classification;
one soft extended in 2XLSS, hard extended in 2XLSSd;
23 point-like in 2XLSS, extended in 2XLSSd;
20 extended in 2XLSS, point-like in 2XLSSd.

Studies of galaxy clusters in the *XMM*–LSS survey have been presented by Adami et al. (2011), Clerc et al. (in preparation) and Willis et al. (2012). More information on confirmed clusters is also available in the *XMM*–LSS survey cluster data base.[9]

4 GENERATION OF THE MULTIWAVELENGTH CATALOGUE

4.1 Input catalogues

Most of the *XMM*–LSS survey area was covered in the $u^\star$, g', r', i', z' bands by the W1 Wide Synoptic field of the CFHTLS. The core area – our G pointings in Table 1, corresponding to the *XMM* Medium Deep Survey (XMDS) – was also covered by the 1 deg^2 Deep field D1. The northernmost strip $\delta \gtrsim -3\overset{\circ}{.}7$ was not part of the CFHTLS and was observed under a Guest Observer programme in a similar configuration at the CFHT (but only in the g', r', z' bands) with three pointings (so-called ABC fields), leaving a gap only in correspondence of the bright star Mira Ceti.

We have used a compilation of the TERAPIX[10] panchromatic catalogues for W1 (release T004) and the ABC fields, edited to remove duplicates in overlapping pointings, and replacing undefined magnitudes resulting from non-detection in one band with the limiting magnitude of the pointing. Separately, we have also used the panchromatic catalogue of the D1 field.

Most of the *XMM*–LSS survey area was also observed by the *Spitzer* Space Telescope, as part of the SWIRE survey (Lonsdale et al. 2003). We obtained from IPAC a compilation of an unpublished release catalogue in the four IRAC (3.6, 4.5, 5.8 and 8.0 μm) and three MIPS (24, 70 and 160 μm) bands. This was preprocessed for classification of extended objects; in particular, IRAC fluxes are Kron fluxes for extended objects and so-called aperture 2 (1.9 arcsec) otherwise, while they are APEX (PRF) fluxes for MIPS.

For the UKIDSS NIR survey, we have retrieved from the WSA public archive[11] data (within 10 arcsec from our X-ray source positions) from the release DR5plus, which at the time provided partial coverage of some areas of the *XMM*–LSS survey via the DXS and UDS surveys (in particular, the latter covers the SXDS area).

For the UV band, we have retrieved from the NASA MAST public *GALEX* archive[12] (using the CASJOBS tool) data from the GR4/GR5 release (within 10 arcsec from our X-ray source positions). Because it is well known that the MAST *GALEX* catalogue contains redundant sources where *GALEX* pointings overlap (so-called tiling artefacts), we have run a procedure to flag *GALEX* objects within 1.5 arcsec from any other one observed in a different tile, and to prefer in each set the one observed in two bands, with smallest interband separation, or with smallest off-axis angle.

The coverage of the *XMM*–LSS survey area by the various catalogues is shown in Fig. 1.

All appropriate data have been included in tables within our data base and elaborated therein with the procedure described below (the optical data were also used separately for the preventive astrometric correction described in Section 3.2).

4.2 Candidate definition procedure

As a preliminary step, within our data base we have constructed correlation tables between the X-ray sources in either 2XLSS or 2XLSSd and each one independently of the CFHTLS D1, W1, SWIRE, UKIDSS and *GALEX* tables, using a radius of 6 arcsec.

The next step is an incremental addition procedure through the above tables in the following order.

(i) We create a generalized correlation table, with columns designated to hold pointers to the various catalogues, initialized with as many records as X-ray sources. Each record is an n-uple (*X*, *D*1, *W*1, *SWIRE*, *UKIDSS*, *GALEX*) initialized as (*X*, 0, 0, 0, 0, 0). Records are termed counterpart sets.

(ii) We start with the D1 table, and for each X-ray source we insert a pointer in the relevant record if there is at least one D1 object within 6 arcsec. If the X-ray source has one optical counterpart only, the D1 pointer is inserted in the existing primary record, so the n-uple is filled as (x_1, d_a, 0, 0, 0, 0).

If it has more, the pointer of the closest candidate is inserted as above, while additional records are added copying from the primary one and replacing the pointer with one associated with the other D1 object [e.g. an additional n-uple (x_1, d_b, 0, 0, 0, 0)].

(iii) Then, we proceed in turn to the next table, inserting an object from such a table when it is closer to one of the existing counterparts in other non-X-ray tables within a predefined radius. Only objects within 6 arcsec from the relevant X-ray source are considered, while a correlation radius of 0.5 arcsec is used when comparing positions of the same origin (i.e. D1 and W1), of 1 arcsec when comparing to

[9] http://xmm-lss.in2p3.fr:8080/l3sdb/
[10] http://terapix.iap.fr/
[11] http://surveys.roe.ac.uk/wsa/
[12] http://galex.stsci.edu/GR4/

SWIRE or UKIDSS catalogues, and of 1.5 arcsec when comparing to *GALEX*.

(iv) A pointer is inserted into an existing record when there is a single match with the X-ray position and all the positions in the previously processed catalogues. For example, an n-uple is updated as (x_1, d_a, w_a, 0, 0, 0). Additional counterpart sets are generated in all other cases (typically an independent counterpart of the X-ray source with no counterpart in previous catalogues, but could also be an ambiguous association of more sources in the current catalogue with a previously defined counterpart set). For example, in the case of W1 objects, they are compared with D1, while SWIRE objects are compared first with W1, then D1, UKIDSS objects are compared with preceding tables (in the order W1, D1, SWIRE) and *GALEX* objects are compared with all other tables (in the order W1, D1, SWIRE, UKIDSS). Therefore, we could end up with completely or partially filled pre-existing n-uples such as (x_1, d_a, w_a, s_a, 0, g_a), with new n-uples such as (x_1, 0, w_n, s_n, u_n, 0) or (x_1, 0, 0, s_p, 0, 0), or (seldom) with ambiguous cases such as (x_1, d_b, w_b, 0, 0, g_q) and (x_1, d_b, w_b, 0, 0, g_r).

(v) Finally, the chance probabilities for random association of a counterpart with the X-ray source are computed as described immediately hereafter.

4.3 Computing probabilities and counterpart ranking

We compute four probabilities: `probXO`, `probXS`, `probXU` and `probXG`. Each is the probability of chance coincidence between the X-ray source and its counterpart in a given catalogue, based on the X-ray to optical (or SWIRE, UKIDSS or *GALEX*) distance, the optical, IR or UV intensity (magnitude or flux) m, and the density of sources brighter than such an intensity. They are based on a formula (Downes et al. 1986) such as

$$prob = 1 - \exp\left[-\pi\ n(\text{brighter than}\, m) r^2\right], \quad (1)$$

where r is the X-ray to counterpart distance, while a rough estimate of the density n(brighter than m) is computed as described in detail in Appendix B.

At this stage, each X-ray source can have more than one potential counterpart (or better, counterpart sets, where each set can include associated counterparts in D1, W1, SWIRE, UKIDSS and *GALEX*). A preliminary ranking can be assigned on coarse probability ranges:

good if $prob < 0.01$;
fair if $0.01 < prob < 0.03$;
bad if $prob > 0.03$.

The acceptable tuning with the data of such a coarse classification is demonstrated by Fig. B1. Such a pre-ranking is refined by a multistep heuristic procedure, which assigns a score based on several criteria, such as assigning higher weights to a good or fair probability in the optical or SWIRE bands, and/or to the fact that the best probability of a counterpart set is at least 10 times better (smaller) than those of any other counterpart set for the same X-ray source, and/or whether the counterpart set is unique, or brightest and closest. In some cases, a visual inspection of the optical thumbnail (see Section 2.4.2.2) with the overlay of all counterpart set elements has been necessary. In exceptional cases, this resulted in a manual editing (usually the deletion of counterpart sets due to artefacts, such as unresolved tiling effects in one of the catalogues, or problems near very bright or saturated sources).

The result of the ranking is the assignment of the value of column `Xrank` (see Table A3) in the multiwavelength catalogues `2XLSSOPT` or `2XLSSOPTd` (derived respectively from the 10-ks and deep X-ray catalogues).

The number of potential counterpart sets can be high (16 813 for `2XLSSOPT` and 20 837 for `2XLSSOPTd`). However, a large number of these (9093 and 11 500), based on the above ranking procedure, obtain a rank `Xrank` $= -1$, which means they have to be rejected. This leaves 7720 or 9337 potential counterpart sets in the publicly released `2XLSSOPT` or `2XLSSOPTd`, respectively. Such non-rejected counterpart sets, as the result of an ambiguity analysis, have `Xrank` between 0 and 2. For X-ray sources with a single counterpart set (either physically unique or just one non-rejected) `Xrank` is either 0 or 1. When an X-ray source has more possible counterpart sets, there is a single one that has `Xrank` $= 0$ or `Xrank` $= 1$ (i.e. the preferred), while all the secondaries have `Xrank` $= 2$. More details on ranks, together with a detailed statistics, are presented in Section 5.2.1. The rank and the potential counterpart list are provided as a convenience for data base users, but are not at all intended as prescriptive. Additional information about visual, spectroscopic and Spectral Energy Distribution (SED) classification of X-ray sources with respect to the optical counterparts can be found in Melnyk et al. (2012).

5 A FEW STATISTICS

5.1 X-ray catalogues

The number of sources in the merged 10-ks catalogue is 5572 for `2XLSS` (4932 in `2XLSSB` and 1923 in `2XLSSCD`). The number of sources in the deep catalogue is 6721 for `2XLSSd` (5881 in `2XLSSBd` and 2645 in `2XLSSCDd`).

The majority of objects detected in the full exposures are confirmed in the 10-ks exposures, usually with the same classification and within a distance of 6 arcsec; the differences are concentrated within the objects with poorer likelihood. However, there are a significant number of detections, not necessarily spurious, which are present either only in the full exposures (not surprising) or even only in the 10-ks exposures. If we consider data before band merging and spurious source filtering, 24 per cent of the soft detections and 40 per cent of the hard detections in full exposures are not confirmed in 10-ks exposures, while 8 per cent (soft) and 19 per cent (hard) 10-ks detections are new.

Considering band-merged data before overlap removal (and spurious source filtering), 29 per cent of the merged detections in full exposures are not confirmed in 10-ks exposures (mainly single soft non-spurious, or in similar proportion between hard and soft when spurious), while 14 per cent of the 10-ks detections are new (the majority are spurious, but mainly single detections in the soft band prevail when non-spurious).

We proceed with a further comparison between the deep and 10-ks catalogues, which allows us to assess a trade-off between deeper but non-uniform exposures and shallower uniform exposures. A comparison with the Version I (`XLSS`) release is given in Appendix C1.

While sources in a catalogue are by construction non-spurious (i.e. with $LH > 15$ in at least one band), they can be detected as such in both bands, detected as non-spurious in one band and spurious in the other, or detected in a single band. The breakdown in percentage is reported in Table 7. The deep catalogue is marginally better for fully fledged detections in both bands.

A breakdown that also considers the classification for the 5117 common objects can be summarized as follows: 85 per cent are classified as point-like identically in both catalogues (which means

Table 7. Basic statistics for the 2XLSS and 2XLSSd catalogues.

Case	2XLSSd	2XLSS
Total number of sources	6721	5572
Detected in both bands		
non-spurious in both bands	27 per cent	23 per cent
non-spurious in soft band only	8 per cent	8 per cent
non-spurious in hard band only	2 per cent	1 per cent
Detected only in soft band	52 per cent	57 per cent
Detected only in hard band	11 per cent	10 per cent
Not detected in other catalogue	24 per cent	9 per cent

either point-like or undetected in each band), and this increases to 97 per cent classified as point-like and compatible (i.e. detected in both bands in one catalogue and in a single band in the other); 2 per cent are classified as extended (usually identically, only compatible in eight cases, while in a single case, the source is detected as extended once in the soft band and once in the hard band); the few remaining cases are 23 2XLSSd and 20 2XLSS extended sources, which are point-like in the other catalogue.

The distances between common objects are in very good agreement: 90 per cent within 2 arcsec, 97 per cent within 4 arcsec and 99 per cent within 6 arcsec (see also Fig. 5c).

Fig. 6 shows a comparison of likelihoods and fluxes for associated sources. As expected, the likelihood in the shorter exposure 2XLSS catalogue is compatible, but lower than the one in 2XLSSd (the points lie below the diagonal fiducial line of equal values).

For fluxes, they are generally consistent (with exceptions for a few extended sources), with only a moderate scatter for fainter objects. With the lack of error bars, we can compare the compatibility of fluxes for the 5144 associated sources between 2XLSSd and 2XLSS. For the 4656 with a soft-band detection in both catalogues, 60, 81 and 96 per cent of the sources have fluxes within 10, 20 and 50 per cent, respectively. The equivalent percentages for the 2146 with a hard-band detection are 53, 77 and 95.

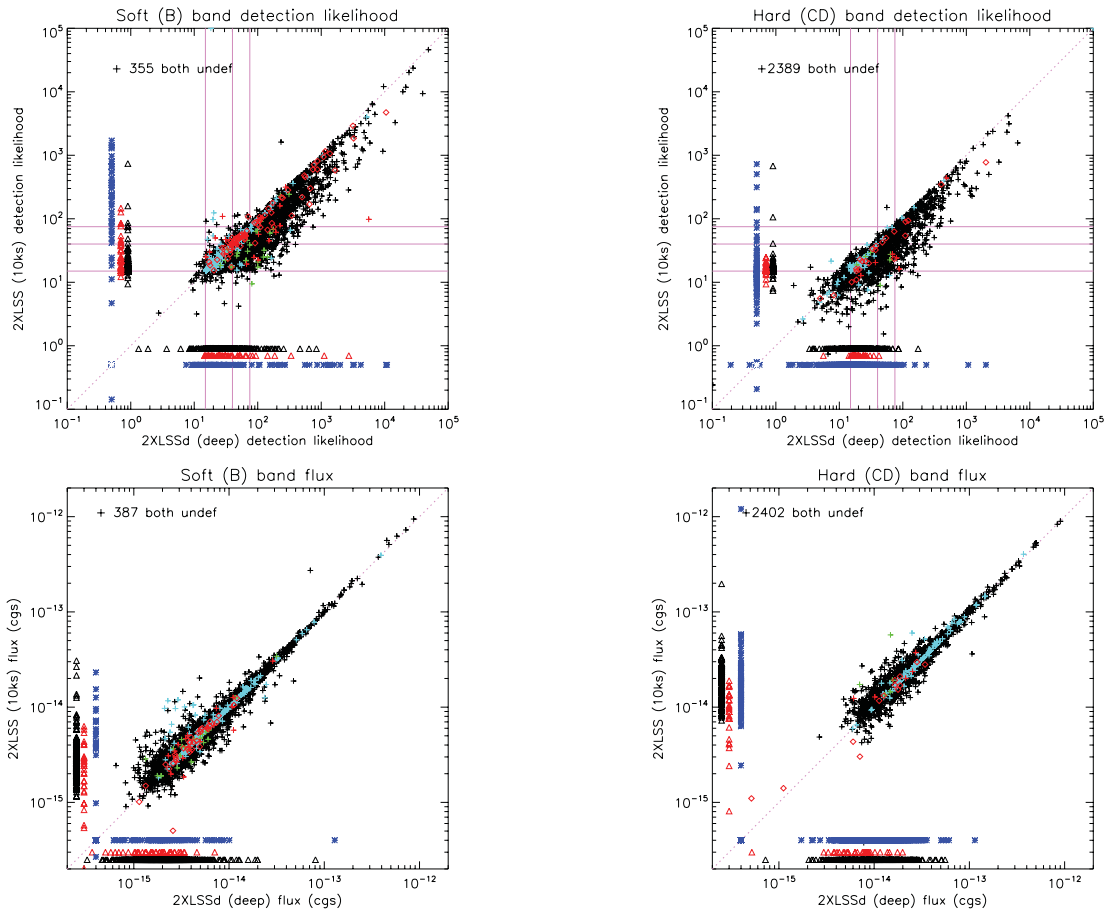

Figure 6. Comparison of the detection likelihood (top row) and of the flux (bottom row) in the soft (left column) and hard (right column) energy bands between 2XLSS and 2XLSSd. Crosses and diamonds indicate point-like or extended objects associated with the two catalogues (see text). Blue asterisks indicate that likelihood or flux are present but undefined in one catalogue, while triangles indicate sources present only in one catalogue (both are placed at a conventional out-of-range *X* or *Y* position). The number of objects with undefined values in both catalogues in a given band, but nevertheless associated, is indicated near the top-left corner of each panel. Colour coding (only in the online version) is as follows: black and cyan crosses denote point-like common sources in 2XLSS good and bad fields, respectively; green crosses denote 2XLSSd extended objects that are point-like in 2XLSS; red crosses denote 2XLSS extended objects that are point-like in 2XLSSd; red diamonds denote extended sources in both 2XLSS and 2XLSSd. Triangles are black or red for point-like or extended sources, which are either new in 2XLSS or present in 2XLSSd but lost in the shallower catalogue. In the likelihood plots, the thin pink lines are fiducial marks corresponding to the spurious/non-spurious threshold (15) and to the conventional 3σ (40) and 4σ (75) levels.

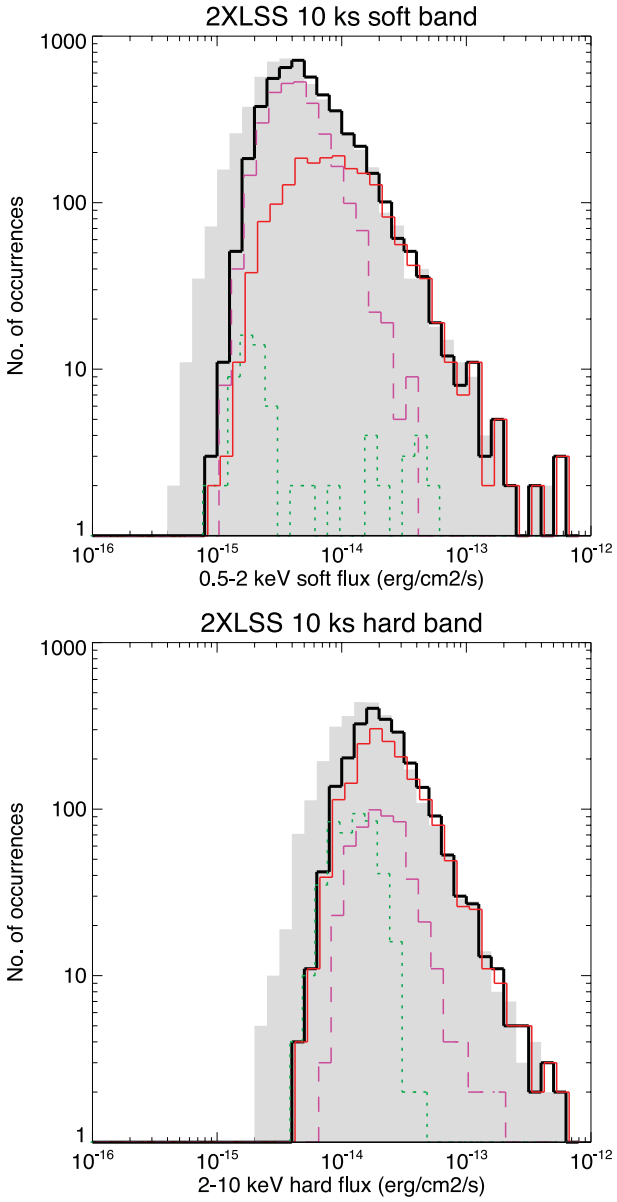

Figure 7. Histogram of the soft (top panel) and hard (bottom panel) fluxes. The grey-shaded histogram in the background refers to the 2XLSSd deep catalogue. All other histograms refer to the 2XLSS 10-ks catalogue, and to all sources in the band (thick black), sources detected in both bands (thin solid red), sources detected only in the band (hence, by definition, non-spurious; thin dashed magenta) and fluxes with a spurious likelihood in the band, associated with a non-spurious source in the other band (thin dotted green). Colours are shown only in the online version. The various histograms are slightly offset for clarity.

In Fig. 7, we also provide a histogram of the fluxes, mainly for the 2XLSS catalogue (but the shaded area indicates what we gain at low fluxes passing from 10 ks to full exposures).

5.2 Multiwavelength catalogues

5.2.1 Statistics on each catalogue

First, we present some general statistics on both catalogues in parallel, quoting values for 2XLSSOPT, followed by those for 2XLSSOPTd in parentheses.

Note that it is necessary to refer to Fig. 1 in order to evaluate whether, in a given region, the reason why we do not find counterparts in a given wavelength table is either because they do not exist or because the region has not been observed at all.

2XLSSOPT (2XLSSOPTd) starts from 16 813 (20 837) nominal counterpart sets, from which we have removed the 9093 (11 500) rejected (Xrank $= -1$ as explained in Section 4.3).

The number of X-ray sources nominally flagged as blank fields (i.e. having a single null counterpart set, which means no catalogued CFHTLS, SWIRE, UKIDSS or *GALEX* counterpart within 6 arcsec) is 221 (248). Note that the absence of catalogued sources does not mean that they are necessarily real blank fields. Often, bright sources are omitted by the catalogues, but are visible if the thumbnail image is inspected. For instance, we can compare the cases of sources 2XLSSOPT.Xseq $= 43302$, which is very close to an $R = 15.6$ galaxy shown in SIMBAD, or 2XLSSOPT.Xseq $= 38678$, whose field is spoiled by the nearby bright star BD-05 427. So, some of the cases flagged as blank fields can instead have a bright counterpart.

With regards to the tentative identifications of 5572 (6721) X-ray sources, we find the following.

18 per cent (17 per cent) have a physically single counterpart (set).

40 per cent (39 per cent) have a single very reliable counterpart (i.e. Xrank $= 0$) plus eventual rejected counterpart sets.

21 per cent (28 per cent) have a single, but not so reliable, counterpart (i.e. Xrank $= 1$), plus eventual rejected counterpart sets.

16 per cent (16 per cent) are pseudo-ambiguous, with one definitely preferred counterpart (Xrank $= 0$), plus one or more nominal secondary counterparts with rank 2.

13 per cent (14 per cent) are definitely ambiguous, with one nominally preferred counterpart (Xrank $= 1$), plus one or more secondary counterparts with rank 2, at least one of which is not much worse than the nominally preferred one.

With reference to the criteria defined in Section 4.3, 48.2 per cent (48.6 per cent) of the sources have a best counterpart with a good probability, 29.5 per cent (30.1 per cent) with a fair probability and 4.0 per cent (3.7 per cent) are nominal blank fields.

We can also relate the counterpart association with the X-ray detection significance (using the cross-calibration between likelihood and number of σ presented in Appendix C3.1). For instance, of the 1412 (1888) X-ray sources detected above 4σ, 77 per cent (76 per cent) have a good counterpart, 18 per cent (20 per cent) a fair counterpart and only 2 per cent (1 per cent) are unidentified; of the 2436 (3169) X-ray sources above 3σ, 68 per cent (65 per cent) have a good counterpart, 25 per cent (27 per cent) a fair counterpart and 2 per cent (2 per cent) are unidentified.

We also note that the ranking depends on the probabilities, and these depend on the distance (Section 4.3) and therefore, ultimately, on the X-ray position. If the latter changes, the rank choice will change. The differences between the two catalogue variants are discussed in Section 5.2.2.

Finally, the quality of the tentative identifications can be assessed from the offset (distance) between the X-ray source position and the position of the best counterpart in the best counterpart set. This is shown in Figs 8 and 5(e). We find that 83 per cent (84 per cent) of all counterparts have a distance within 4 arcsec, which occurs for 90 per cent (91 per cent) of the best counterparts with fair or good probabilities (the circles in Fig. 8) and for 95 per cent (95 per cent) of those with good probabilities (the filled circles in Fig. 8).

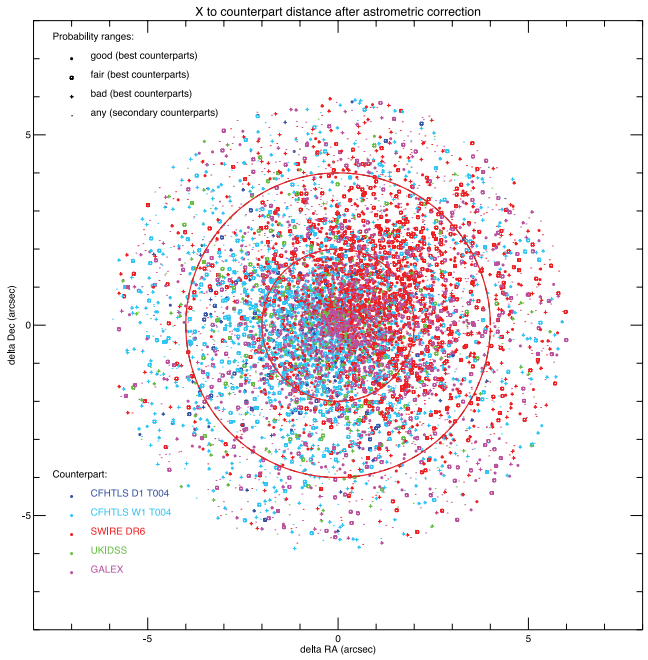

Figure 8. Distances in RA and Dec. between the X-ray corrected position and the counterpart position. Different symbols indicate the identification quality. A circle is plotted when the counterpart is the best one, and the chance probability is good or fair (filled in case of good probability). A cross is plotted for the best counterpart when the probability is bad. A dot is plotted for secondary (ambiguous) counterparts, irrespective of probability, but only if it is good or fair. Different colours (online version only) or shades (as shown in the figure) indicate the origin of the counterpart position for the distance calculation. Two fiducial radii of 2 and 4 arcsec are also shown. This figure refers to `2XLSS`; the equivalent figure for `2XLSSd` is extremely similar.

There is some evidence from Fig. 8 of systematics in the deviations between X-ray positions and positions in the various catalogues. The average deviation for the optical and UKIDSS catalogues clusters around a point in the third quadrant (e.g. −0.39, −0.07 arcsec for W1), while the one for SWIRE clusters around a point in the first quadrant (0.82, 0.57 arcsec). For `2XLSSd`, they are (−0.40, −0.07 arcsec) and (0.79, 0.52 arcsec), respectively.

Fig. 5(e) reports the distribution of the X-ray to counterpart distance, using as the counterpart position the one with the smallest distance (in 37, 34, 9 and 20 per cent of cases, these are optical, SWIRE, UKIDSS and *GALEX* sources, respectively).

5.2.2 *Differences between `2XLSSOPT` and `2XLSSOPTd`*

There are three main reasons for the differences between the two catalogues with optical identifications, the first two can be considered physiological because of the different exposure times:

(i) the X-ray source can be detected in one of the input catalogues and not in the other;

(ii) the X-ray source can be detected or classified differently (spurious or non-spurious, in one or two bands, point-like or extended);

(iii) the X-ray source can be detected at a displaced position.

The latter displacement could result in some of the possible counterparts being outside the 6-arcsec correlation radius, and therefore included in the list of counterpart sets being partially or totally different, and with different ranks.

Considering all potential counterpart sets (including negative rank rejected counterparts, because rejection might act differently as a result of the displacement), about 86 per cent of the common ones are identical (i.e. they have the same counterparts in all non-X-ray catalogues), of which 139 are confirmed blank fields (i.e. no catalogued counterpart in any waveband). The remaining cases might be altogether different counterpart sets, or might partially match (in some of the non-X-ray catalogues). More details are provided in Appendix C2.

Concerning the tentative blank fields, we should note that, besides the 139 common ones, there are 109 `2XLSSOPTd` blank fields not present in the 10-ks catalogue and 82 `2XLSSOPT` blank fields that are new in the latter catalogue (42 are new X-ray sources with no deep counterpart, and the other 40 are no longer blank fields).

Coming now to non-blank fields, remember that the identification procedure is incremental. So, it starts (in the absence of a D1 counterpart) associating a W1 object with the X-ray source. Then, it might append one SWIRE object (associated with the X-ray source and within 1 arcsec from W1) to the counterpart set, and create a new counterpart set for another SWIRE object, and so on and so forth for the other wavebands. Each association could be different as a result of a small displacement in the X-ray position. In the most favourable case, this might just prefer a particular counterpart in a counterpart set otherwise identical and identically ranked. In other cases, counterpart sets similar but differing in one waveband might be ranked differently (primary versus secondary, or even rejected).

5.3 Comparison with XMDS

In this section, we provide a sketchy comparison between the catalogues presented in this paper and the XMDS catalogue, a subset of which was published as the XMDS/VVDS 4σ catalogue (Chiappetti et al. 2005). Because the entire XMDS catalogue is unpublished, we will release it through our data base contextually with the Version 2 *XMM*–LSS catalogues (see Table 2). A comparison provides an opportunity to validate and cross-calibrate two different pipelines – a traditional one and an innovative one – on the same input data. The main differences between the two pipelines, and further details of the comparison, are reported in Appendix C3.

The XMDS catalogue includes 1168 sources (by definition, all in the G-labelled fields), of which 1057 are catalogued in `2XLSSd`. Appendix C3.1 provides further details, in particular the following.

(i) A cross-calibration of the detection likelihood of XAMIN, with the significance in terms of the number of σ of the XMDS, shows that a likelihood of 75 corresponds more or less to the 4σ level, and one of 40 to the 3σ level.

(ii) Fluxes match well, although with a systematic difference (which, considering the different procedures, is fully acceptable). That is, `2XLSSd` fluxes are 0.895 lower than the XMDS ones in the B band, while they are only 1.040 higher in the CD band.

(iii) Also, XMDS fluxes measured simultaneously in all bands match well the `2XLSSd` fluxes measured separately for sources detected in both bands. This reinforces trust in the band-merging procedure described in Section 3.3.

It is also possible to compare the counterparts in optical (and other) bands between the XMDS and the `2XLSSOPTd` catalogue. As shown in Appendix C3.2, the compatibility between the counterparts is also satisfactory.

5.4 Comparison with 2XMM

We have perfomed a quick comparison with the second *XMM*–Newton serendipitous source (2XMM) catalogue (Watson et al. 2009). Details are reported in Appendix C4. Despite the differences in the data processing and in the definition of the energy band, we find an acceptable match in terms of the number of sources, respective distance and fluxes.

6 CONCLUDING REMARKS

In this paper, we have presented the X-ray full-exposure (`2XLSSd`) and 10-ks limited exposure (`2XLSS`) catalogues for the 11.1 deg^2 *XMM*–LSS field. The total number of X-ray sources reported in these two catalogues are 6721 and 5572, respectively. The sources were detected in the 0.5–2 and/or 2–10 keV energy bands with a new version (3.2) of the XAMIN pipeline. We have also provided two multiwavelength catalogues (cross-correlating the X-ray sources with IR/SWIRE, NIR/UKIDSS, optical/CFHTLS and UV/*GALEX* sources), `2XLSSOPTd` and `2XLSSOPT`, corresponding to the full and 10-ks limited exposure catalogues respectively. We have also described in detail the X-ray band merging, the X-ray point-like and extended source classification, the matching procedure of counterparts from multiwavelength surveys, as well as extensive statistics to compare the two presented catalogues with each other and with previous studies.

Catalogues and associated data products are available through the Milan data base (http://cosmosdb.iasf-milano.inaf.it/XMM-LSS/), with a reduced summary stored at the CDS.

ACKNOWLEDGMENTS

The results presented here are based on observations obtained with *XMM–Newton*, a European Space Agency (ESA) science mission with instruments and contributions directly funded by ESA Member States and NASA.

We acknowledge the work carried out by Krys Libbrecht on the XAMIN pipeline translation.

Optical photometry data were obtained with MegaPrime/MegaCam, a joint project of CFHT and CEA/DAPNIA, at the CFHT, which is operated by the National Research Council (NRC) of Canada, the Institut National des Sciences de l'Univers of the Centre National de la Recherche Scientifique (CNRS) of France, and the University of Hawaii. This work is based in part on data products produced at TERAPIX and the CADC as part of the CFHTLS, a collaborative project of NRC and CNRS. We acknowledge the help of J. J. Kavelaars of the CADC Help Desk concerning the thumbnail cutout for the ABC fields.

This work is in part based on observations made with the *Spitzer* Space Telescope, which is operated by the Jet Propulsion Laboratory, California Institute of Technology under NASA. Support for this work, part of the *Spitzer* Space Telescope Legacy Science Programme, was provided by NASA through an award issued by the Jet Propulsion Laboratory, California Institute of Technology under NASA contract 1407.

This work is in part based on data collected within the UKIDSS survey. The UKIDSS project uses the UKIRT Wide Field Camera funded by the UK Particle Physics and Astronomy Research Council (PPARC). Financial resources for WFCAM Science Archive development were provided by the UK Science and Technology Facilities Council (STFC; formerly by PPARC).

GALEX is a NASA mission managed by the Jet Propulsion Laboratory. The *GALEX* data used in this paper were obtained from the Multimission Archive at the Space Telescope Science Institute (MAST). STScI is operated by the Association of Universities for Research in Astronomy, Inc., under NASA contract NAS5–26555. Support for MAST for non-*HST* data is provided by the NASA Office of Space Science via grant NNX09AF08G and by other grants and contracts.

OM, AE and JS acknowledge support from the ESA PRODEX Programmes "XMM–LSS" and "XXL", and from the Belgian Federal Science Policy Office. They also acknowledge support from the Communauté Française de Belgique – Actions de recherche concertés – Académie universitaire Wallonie-Europe".

REFERENCES

Adami C. et al., 2011, A&A, 526, A18
Baldi A., Molendi S., Comastri A., Fiore F., Matt G., Vignali C., 2002, ApJ, 564, 190
Bertin E., Arnouts S., 1996, A&AS, 117, 393
Chiappetti L. et al., 2005, A&A, 439, 413
Clerc N., Sadibekova T., Pierre M., Pacaud F., Le Fèvre J.-P., Adami C., Altieri B., Valtchanov I., 2012, MNRAS, 423, 3561
Downes A. J. B., Peacock J. A., Savage A., Carrie D. R., 1986, MNRAS, 218, 31
Elyiv A. et al., 2012, A&A, 537, A131
Lawrence A. et al., 2007, MNRAS, 379, 1599
Lonsdale C. J. et al., 2003, PASP, 115, 897
Martin D. C. et al., 2005, ApJ, 619, L1
Melnyk et al., 2012, A&A, submitted
Pacaud F. et al., 2006, MNRAS, 372, 578
Paioro L., Chiappetti L., Garilli B., Franzetti P., Fumana M., Scodeggio M., 2008, in Argyle R. W., Bunclark P.S., Lewis J. R., eds, ASP Conf. Ser. Vol. 394, Astronomical Data Analysis Software and Systems. Astron. Soc. Pac., San Francisco, p. 397
Pierre M. et al., 2004, J. Cosmol. Astropart. Phys., 9, 11
Pierre M. et al., 2007, MNRAS, 382, 279 (Paper I)
Ueda Y. et al., 2008, ApJS, 179, 124
Watson M. G. et al., 2009, A&A, 493, 339
Willis et al., 2012, MNRAS, doi:10.1093/mnras/sts540

APPENDIX A: LISTINGS OF DATA BASE CONTENT

The list of columns in the X-ray single-band and band-merged tables is almost the same as in Paper I, but these are reported for completeness in Tables A1 and A2. Just as for Paper I, the main parameters (as flagged in such tables) of the merged X-ray catalogue are also available in electronic form at the CDS. However, the multiwavelength tables have a substantially increased number of columns, which are listed in Table A3.

APPENDIX B: DETAILS OF PROBABILITY COMPUTATION

Probabilities of chance association between a counterpart and an X-ray source are computed using equation (1), where the density n (brighter than m) is computed from simple linear fits, as reported in Table B1. This table also indicates the magnitudes or fluxes used to look up the density for the appropriate band. We have only made a rough estimate of the parametrization of the

Table A1. List of parameters provided in the public *XMM*–LSS catalogues. All are available at the *XMM*–LSS Milan data base in the separate tables `2XLSSB` or `2XLSSBd` for the soft band and `2XLSSCD` or `2XLSSCDd` for the hard band. The column name has an appropriate prefix, as follows. When there are two column names given, one with the prefix B and one with the prefix CD, only the one applicable to the given band appears in the relevant table, but both might show up in the band-merged tables `2XLSS` or `2XLSSd` (the family of tables `2XLSSd`, `2XLSSBd` and `2XLSSCDd` constitutes the full exposure catalogue, while `2XLSS`, `2XLSSB` and `2XLSSCD` are the 10-ks catalogue). Column names without a prefix are relevant to the individual band only. The last four columns indicate the following: (X) whether a parameter is natively computed by XAMIN; (m) whether a parameter is available also in the band-merged table; (o) whether a parameter is present in the multiwavelength table together with those described in Table A3; (C) whether a parameter is present in the catalogue stored at the CDS.

Column name	Units	Meaning and usage	X	m	o	C
`Bseq or CDseq`	–	Internal sequence number (unique)		X	X	X
`Bcatname or CDcatname`	–	IAU catalogue name `2XLSS`*x*`Jhhmmss.s-ddmmss`, *x*=`B or CD`		X	X	X
`Xseq`	–	Numeric pointer to merged entry (see Table A2)		X	X	X
`Xcatname`	–	Name pointer to merged entry (see Table A2)		X	X	X
`Xlsspointer`	–	`Xseq` of corresponding source in `XLSS` version I catalogue		X	X	X
`Xdeep`	–	`Xseq` of corresponding source in `2XLSSd` (in table `2XLSS` only)		X	X	X
`Xfield`	–	*XMM* pointing number (internal use)		X	X	
`FieldName`	–	*XMM* pointing name		X	X	
`Xbadfield`	0 or 1	Pointing is good (0) or bad (1)		X	X	
`expm1`	s	MOS1 camera exposure in the band	X			
`expm2`	s	MOS2 camera exposure in the band	X			
`exppn`	s	The pn camera exposure in the band	X			
`gapm1`	arcsec	MOS1 distance to nearest gap	X			
`gapm2`	arcsec	MOS2 distance to nearest gap	X			
`gappn`	arcsec	The pn distance to nearest gap	X			
`Bnearest or CDnearest`	arcsec	Distance to nearest detected neighbour	X	X		
`Bc1c2`	0|1|2	1 for class C1, 2 for C2, 0 for undefined		X	X	X
`CDc1c2`	0|1|2	1 for class C1, 2 for C2, 0 for undefined				
`Bcorerad or CDcorerad`	arcsec	Core radius EXT (for extended sources)	X	X		X
`Bextlike or CDextlike`	–	Extension likelihood EXT_LH	X	X		X
`Bdetlik_pnt or CDdetlik_pnt`	–	Detection likelihood DET_LH for point-like fit	X			
`Bdetlik_ext or CDdetlik_ext`	–	Detection likelihood DET_LH for extended fit	X			
`Boffaxis or CDoffaxis`	arcmin	Off-axis angle		X		X
`Brawra_pnt or CDrawra_pnt`	°	Source RA (not astrometrically corrected) for point-like fit	X			
`Brawdec_pnt or CDrawdec_pnt`	°	Source Dec. (not astrometrically corrected) for point-like fit	X			
`Brawra_ext or CDrawra_ext`	°	Source RA (not astrometrically corrected) for extended fit	X			
`Brawdec_ext or CDrawdec_ext`	°	Source Dec. (not astrometrically corrected) for extended fit	X			
`Bra_pnt or CDra_pnt`	°	Source RA (astrometrically corrected) for point-like fit	X			
`Bdec_pnt or CDdec_pnt`	°	Source Dec. (astrometrically corrected) for point-like fit	X			
`Bra_ext or CDra_ext`	°	Source RA (astrometrically corrected) for extended fit	X			
`Bdec_ext or CDdec_ext`	°	Source Dec. (astrometrically corrected) for extended fit	X			
`Bposerr or CDposerr`	arcsec	Error on coordinates according to Table 4		X		X
`Bratemos_pnt or CDratemos_pnt`	count s^{-1}	MOS count rate for point-like fit	X			
`Bratepn_pnt or CDratepn_pnt`	count s^{-1}	The pn count rate for point-like fit	X			
`Bratemos_ext or CDratemos_ext`	count s^{-1}	MOS count rate for extended fit	X			
`Bratepn_ext or CDratepn_ext`	count s^{-1}	The pn count rate for extended fit	X			
`countmos_pnt`	count	MOS number of counts for point-like fit	X			
`countpn_pnt`	count	The pn number of counts for point-like fit	X			
`countmos_ext`	count	MOS number of counts for extended fit	X			
`countpn_ext`	count	The pn number of counts for extended fit	X			
`bkgmos_pnt`	ct/pixel/detector	MOS local background for point-like fit	X			
`bkgpn_pnt`	ct/pixel	The pn local background for point-like fit	X			
`bkgmos_ext`	ct/pixel/detector	MOS local background for extended fit	X			
`bkgpn_ext`	ct/pixel	The pn local background for extended fit	X			
`Bflux or CDflux`	erg cm^{-2} s^{-1}	Source flux (undefined; i.e. −1 for extended)		X		X
`Bfluxflag or CDfluxflag`	0 to 2	0 if MOS–pn difference <20 per cent, 1 between 20 and 50 per cent, 2 above 50 per cent		X		X

density for the entire *XMM*–LSS area, neglecting any possible spatial variation.

The X-ray to CFHTLS probability, called `probXO`, is computed for sources with a CFHTLS counterpart in the order: D1 if present, else W1. In the case of undefined CFHTLS magnitudes, the pointing tile limiting magnitude was used (as read directly from the W1 table, or fixed to $i' = 25$ for D1).

The other probabilities, X-ray to SWIRE probability `probXS`, X-ray to UKIDSS probability `probXU` and X-ray to GALEX probability `probXG`, are computed as given in the notes in Table B1.

A probability of 99 (undefined) is assigned whenever it could not be computed.

The statistics of the probability ranking defined in Section 4.3 is shown in Fig. B1. This figure indicates an acceptable tuning with the

Table A2. List of data base parameters, as in Table A1, but for the additional columns present only in the merged catalogue tables `2XLSS` or `2XLSSd`. When there are two column names given, one with the prefix B and one with the prefix CD, they relate to the given band, and both show up in the band-merged table. Column names with the prefix X are relevant to merged properties.

Column name	Units	Meaning and usage	X	m	o	C
`Xseq`	–	Internal sequence number (unique)		X	X	X
`Xcatname`	–	IAU catalogue name `2XLSS`*d*`Jhhmmss.s-ddmmss`*c*, see Section 3.5		X	X	X
`Bspurious and CDspurious`	0 or 1	Set to 1 when soft/hard component has DET_LH<15		X		
`Bdetlike and CDdetlike`	–	Detection likelihood EXT_LH (pnt or ext according to source class)	X	X		X
`Xra`	°	Source RA (astrometrically corrected) (pnt or ext acc. to source class in best band)		X	X	X
`Xdec`	°	Source Dec. (astrometrically corrected) (pnt or ext acc. to source class in best band)		X	X	X
`Bra and CDra`	°	Source RA (astrometrically corrected) (pnt or ext according to source class)		X	X	X
`Bdec and CDdec`	°	Source Dec. (astrometrically corrected) (pnt or ext according to source class)		X	X	X
`Xbestband`	2 or 3	Band with highest likelihood: 2 for B, 3 for CD		X		
`Xastrocorr`	4 or 5	Astrometric correction from CFHTLS (4) or USNO (5) or none (0)		X		
`Xmaxdist`	arcsec	Distance between B and CD positions		X		
`Xlink`	–	Pointer to `Xseq` of secondary association (see Section 3.5)		X		
`Bratemos and CDratemos`	count s^{-1} per detector	MOS count rate (pnt or ext according to source class)	X	X		X
`Bratepn and CDratepn`	count s^{-1}	The pn count rate (pnt or ext according to source class)	X	X		X

Table A3. List of additional non-X-ray columns in the multiwavelength `2XLSSOPT` or `2XLSSOPTd` tables. These also include columns with the X, B or CD prefixes from Tables A1 and A2, while those with the O, S, U or G prefix refer to optical, SWIRE, UKIDSS or *GALEX* data. Those without a prefix refer to combined properties.

Column name	Units	Meaning and usage
`Xrank`	−1 0 1 2	Ranking of the counterpart set (see 4.3)
`Ou`	magnitude	$u^\star$ magnitude
`Og`	magnitude	g' magnitude
`Or_`	magnitude	r' magnitude
`Oi`	magnitude	i' magnitude
`Oz`	magnitude	z' magnitude
`Ou_e`	magnitude	Error on $u^\star$ magnitude
`Og_e`	magnitude	Error on g' magnitude
`Or_e`	magnitude	Error on r' magnitude
`Oi_e`	magnitude	Error on i' magnitude
`Oz_e`	magnitude	Error on z' magnitude
`OseqD1`	–	Internal sequence number (if magnitudes from D1 field)
`OseqW1`	–	Internal sequence number (in W1 or ABC fields)
`Ofield`	–	CFHT field identification in form $\pm x \pm y$ or D1 or A,B,C (see 4.1 and Fig. 1)
`Ora`	°	RA of the optical candidate
`Odec`	°	Dec. of the optical candidate
`Oflag`	–	Binary flag combining 0/1 galaxy/star, 0/4 normal/masked, 0/8 normal/saturated
`Sf36`	μJy	IRAC flux at 3.6 μm
`Sf45`	μJy	IRAC flux at 4.5 μm
`Sf58`	μJy	IRAC flux at 5.8 μm
`Sf80`	μJy	IRAC flux at 8.0 μm
`Sf24`	μJy	MIPS flux at 24 μm
`Sf70`	μJy	MIPS flux at 70 μm
`Sf160`	μJy	MIPS flux at 160 μm
`Sf36_e`	μJy	Error on 3.6 μm flux
`Sf45_e`	μJy	Error on 4.5 μm flux
`Sf58_e`	μJy	Error on 5.8 μm flux
`Sf80_e`	μJy	Error on 8.0 μm flux
`Sf24_e`	μJy	Error on 24 μm flux
`Sf70_e`	μJy	Error on 70 μm flux
`Sf160_e`	μJy	Error on 160 μm flux
`Sseq`	–	Internal sequence number for SWIRE objects
`Sra`	°	RA of the SWIRE candidate
`Sdec`	°	Dec. of the SWIRE candidate
`Uj`	magnitude	*J* magnitude
`Uh`	magnitude	*H* magnitude
`Uk`	magnitude	*K* magnitude
`Uj_e`	magnitude	Error on *J* magnitude
`Uh_e`	magnitude	Error on *H* magnitude
`Uk_e`	magnitude	Error on *K* magnitude

Table A3 – *continued*

Column name	Units	Meaning and usage
`Useq`	–	Internal sequence number for UKIDSS objects
`Ura`	°	RA of the UKIDSS candidate
`Udec`	°	Dec. of the UKIDSS candidate
`Gnuv`	mJy	*GALEX* near-UV (NUV) flux
`Gfuv`	mJy	*GALEX* far-UV (FUV) flux
`Gnuv_e`	mJy	Error on NUV flux
`Gfuv_e`	mJy	Error on FUV flux
`Gseq`	–	Internal sequence number for *GALEX* objects
`Gra`	°	RA of the *GALEX* candidate
`Gdec`	°	Dec. of the *GALEX* candidate
`distXO`	arcsec	Distance from the X-ray corrected position to the optical position
`distXS`	arcsec	Distance from the X-ray corrected position to the SWIRE position
`distXU`	arcsec	Distance from the X-ray corrected position to the UKIDSS position
`distXG`	arcsec	Distance from the X-ray corrected position to the *GALEX* position
`probXO`	–	Chance probability of X-ray to optical association (see Section 4.3)
`probXS`	–	Chance probability of X-ray to SWIRE association (see Section 4.3)
`probXU`	–	Chance probability of X-ray to UKIDSS association (see Section 4.3)
`probXG`	–	Chance probability of X-ray to *GALEX* association (see Section 4.3)

Table B1. Parameters used for probability computation.

Probability	m	Density n (brighter than m)	a	b	Notes
probXO	i'	$n(<i') = 10^{a+bi'}$	−9.32415	0.293833	For D1 field
			-9.23183	0.290519	For W1 excluding ABC fields
	r'	$n(<r') = 10^{a+br'}$	−9.18619	0.279706	For W1 ABC fields
probXS	F_λ	$n(>F_\lambda) = 10^{a+b*\log(F_\lambda)}$			In increasing order of λ whichever first
	$\lambda = 3.6$ μm		−1.68062	−0.944191	
	$\lambda = 4.5$ μm		−1.73693	−0.976644	
	$\lambda = 5.8$ μm		−2.04933	−0.829700	
	$\lambda = 8.0$ μm		−1.49944	−1.07201	
	$\lambda = 24$ μm		0.102480	−1.53410	
probXU	J	$n(<J) = 10^{a+bJ}$	−8.67503	0.268272	Taken as best if both bands are present
	K	$n(<K) = 10^{a+bK}$	−8.96264	0.321560	
probXG	NUV	$n(<\text{NUV}) = 10^{a+b\text{NUV}}$	−11.0875	0.326965	Taken as best if both bands are present
	FUV	$n(<\text{FUV}) = 10^{a+b\text{FUV}}$	−13.9827	0.433838	

CFHTLS, SWIRE and UKIDSS catalogues, while the *GALEX* data are perhaps overtuned, in the sense that there is an excess of good probabilities. This could indicate that the probability computation has to be revised.

APPENDIX C: COMPARISON BETWEEN CATALOGUES

Here, we provide details on the comparisons between `2XLSSd` and Version I `XLSS` (Section C1), between `2XLSSOPT` and `2XLSSOPTd` (Section C2), between our catalogues and the XMDS catalogue (Section C3) and between our catalogues and the 2XMM catalogue (Section C4).

C1 Comparison between `XLSS` and `2XLSSd`

First, we have checked that the new pipeline version provides results consistent with the previous IDL version by performing detailed tests on simulated and real *XMM* pointings. The detection parts of both pipelines give nearly identical results for point-like and extended sources. The characterization parts (maximum likelihood fitting) are in excellent agreement for point-like sources. Regarding extended sources, comparisons of fluxes, sizes and likelihood estimates from the two pipelines are in very good agreement, although some differences do show up for individual faint sources or sources close to the detector borders and gaps. These differences can be attributed to statistical fluctuations. By comparing these values to the input characteristics of simulated sources in a statistical sense, we conclude that both pipelines perform equivalently. Finally, we have directly compared the results.

The association between sources in the Version 2 catalogues (`2XLSS` and `2XLSSd`) with the earlier `XLSS` release (in the smaller area covered by the latter) is possible using the data base column `Xlsspointer`, as explained in Section 3.5. There are 2824 sources common between `XLSS` and `2XLSSd` (out of 3385 in `XLSS`). There are 452 objects appearing only in `2XLSSd` in the pointings covered by `XLSS` and there are 561 `XLSS` objects not confirmed in `2XLSSd`. A majority (95 per cent of the former and 88 per cent of the latter) have a poor detection likelihood ($LH < 40$ corresponding conventionally to $<3\sigma$). As an example of the good agreement between the two catalogue versions (mainly between the older and newer XAMIN versions, and also between the 6 versus 10 arcsec band merging), we compare the fluxes between `XLSS` and `2XLSSd` (which makes sense because `XLSS` also used full exposures), via the plots given in Fig. C1.

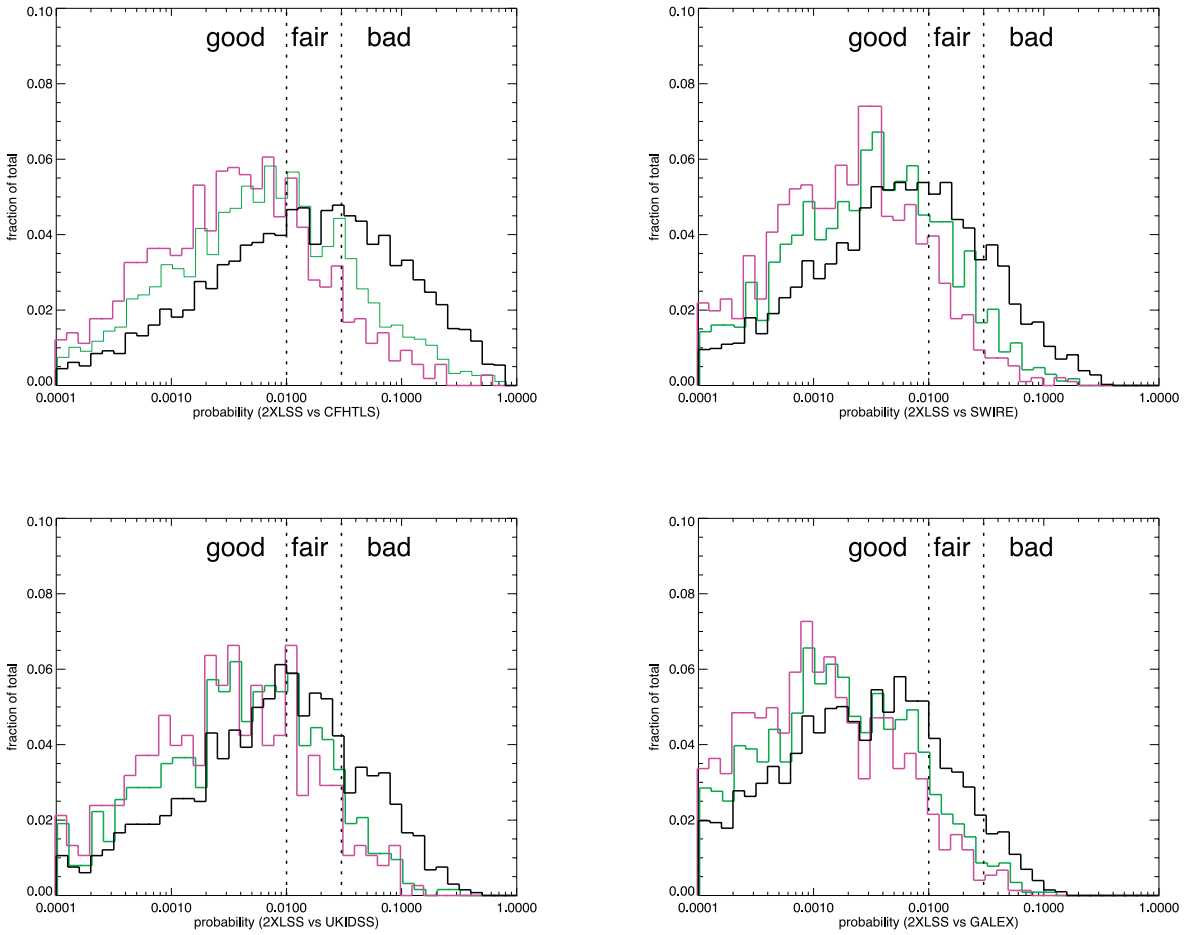

Figure B1. Histograms of the four probabilities (`probXO`, `probXS`, `probXU` and `probXG`) normalized to the total number of best counterparts without any undefined probability in the total sample (thick black), with a detection likelihood of at least 40 (3σ) in the best band (thin light-grey line; green in the online version), or of at least 75 (4σ, thick dark-grey line; magenta in the online version). The dashed fiducial lines identify the loci with good, fair or bad probability, as defined in Section 4.3.

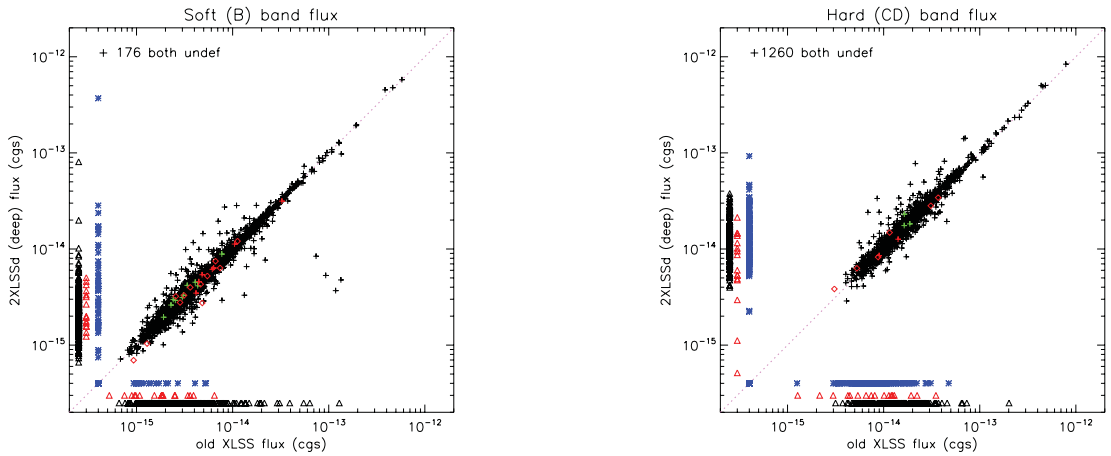

Figure C1. Comparison of the flux in the soft (left column) and hard (right column) energy bands between the Version I `XLSS` catalogue and `2XLSSd`. Symbols are identical to those of Fig. 6.

C2 Comparison between `2XLSSOPT` and `2XLSSOPTd`

There are 20 837 potential counterpart sets for 6721 X-ray sources in input for `2XLSSOPTd`, and 16 813 for 5572 sources for `2XLSSOPT` (the comparison includes negative rank rejected counterparts, because rejection might act differently because of the displacement). Of these, 1188 entries (for 428 X-ray sources) in `2XLSSOPT` have no obvious correspondent in the deep `2XLSSOPTd`.

15 625 counterpart sets are associated with 5144 X-ray sources in 2XLSS with a corresponding source in 2XLSSd. These are the X-ray sources present in both catalogues.

There are 13 454 counterpart sets (86 per cent of the common ones) for 4979 2XLSS sources (97 per cent of the common ones) that are identical (i.e. they have the same counterparts in all non-X-ray catalogues).

Of these, 139 are confirmed blank fields (no catalogued counterpart in any waveband).

Of the remaining 13 315, 11 556 (87 per cent) have the same rank in 2XLSSOPTd and 2XLSSOPT (i.e. with reference to the rank definitions in Section 4.3):

3710 are primary counterparts;
1439 are secondary counterparts;
6407 are rejected counterparts, not included in the catalogues;
1759 (of the 13 315) have the same counterpart but with a different rank:
for 511 of them, the rank change is irrelevant (i.e. they remain the primary counterpart in both catalogues);
201 and 175 counterpart sets rejected in 2XLSSOPTd are respectively primary and secondary choices in 2XLSSOPT;
170 and 196 primary or secondary choices in 2XLSSOPTd are rejected in 2XLSSOPT;
254 2XLSSOPTd primaries become secondary in 2XLSSOPT, while 252 undergo the opposite change from secondary to primary.

In 38 additional cases (only 0.2 per cent of the common ones), the counterpart set is the same between a couple of 2XLSSOPT and 2XLSSOPTd entries, but the latter are not associated by column Xdeep. That is, two sources have the same counterpart set but are not the closest. In 10 cases, this is because of ambiguous band merging, but in the rest (which is an extremely small number) this probably means that there are two 10-ks sources both displaced from but close to a given full exposure one (or vice versa).

The 2171 remaining 2XLSSOPT counterpart sets (covering 1479 individual 2XLSS X-ray sources) can be altogether different from all counterpart sets in 2XLSSOPTd for the associated X-ray source (the X-ray source position has moved so much that entire counterpart sets are farther than 6 arcsec from either position), or might partially match (from one to four out of the five D1, W1, SWIRE, UKIDSS or GALEX catalogues).

A breakdown of the partial matches (with a total larger than 2171, because one specific counterpart set is compared with all the 2XLSSOPTd counterpart sets for the corresponding X-ray source) is:

2150 are no matches;
234 cases match in one catalogue;
66 cases match in two catalogues;
25 in three catalogues;
7 in four catalogues.

An alternative breakdown (totalling 2171) is the following:

261 single no-match cases;
1601 multiple no-matches per X-ray source;
15 cases with one counterpart set with one-to-three catalogue matches;
51 cases with one no-match and another one-to-three catalogue matches;
6 cases with mixed matches;
237 with more no-match and mixed matches.

A different approach for the comparison is to consider only the best counterparts i.e. those ranked 0–1 (by definition, one per X-ray source). Let us exclude the 1607 2XLSSOPTd (24 per cent of 6721) X-ray sources not confirmed in the 10-ks catalogue, and the 528 2XLSSOPT (8 per cent of 5572) new sources in the 10-ks catalogue, and let us concentrate on the common sources. Of their best counterparts:

≈86 per cent are essentially confirmed in both catalogues:

3 per cent are confirmed tentative blank fields;
72 per cent have the same counterparts and the same rank;
10 per cent have the same counterparts and compatible ranks;
only 1.4 per cent have partially matching counterpart sets with the same or compatible best rank.

A further 5 per cent and 4 per cent have the same counterparts but they are ranked differently (the best counterpart in one catalogue is either secondary or rejected in the other).

The remaining 5 per cent have altogether different or partially matching counterparts, which are ranked differently.

So, the difference between counterparts in the deep and 10-ks catalogues is confined to less than 15 per cent of the common sources.

C3 Comparison with XMDS

A subset of the XMDS data was published as the XMDS/VVDS 4σ catalogue (Chiappetti et al. 2005; the same paper contained also the $\log N$–$\log S$ of the entire catalogue). Contextually to the release of the entire XMDS catalogue through our data base together with Version 2 *XMM*–LSS catalogues (see Table 2), here we report on some details of a comparison between the catalogues presented in this paper (mainly 2XLSSd) and XMDS.

The main procedural differences between the two pipelines can be summarized as follows.

(i) The XMDS covers the fields G01 to G19 in Table 1.
(ii) XMDS data have been analysed with a fully independent (and more traditional) pipeline based on the one by Baldi et al. (2002).
(iii) The XMDS pipeline uses in a first step SAS to detect candidates in five energy bands simultaneously (and not in two independent bands with later merging) operating on event files merged from all three *XMM* cameras and from the entire *XMM* field of view (not just the central 13 arcmin).
(iv) In the next step it applies the Baldi et al. (2002) characterization, which is robust but oriented to point sources only (unlike the wavelet method in XAMIN, which handles better extended sources).
(v) The event pattern selection is different (non-standard and broader in XMDS).
(vi) The removal of redundant sources is handled differently. In particular, the primary detection is chosen differently, the position is inherited from the primary detection, but the flux is obtained stacking data from all overlapping pointings.
(vii) The astrometric correction offsets are different.
(viii) The XMDS catalogue does not include spurious objects (but only those above a probability threshold), so the difference between the raw data base table and the catalogue is only a result of the overlap removal procedure.

C3.1 Comparison of the X-ray source lists

As anticipated in Section 5.3, the XMDS catalogue includes 1168 sources, by definition all in the G-labelled fields. Comparison with

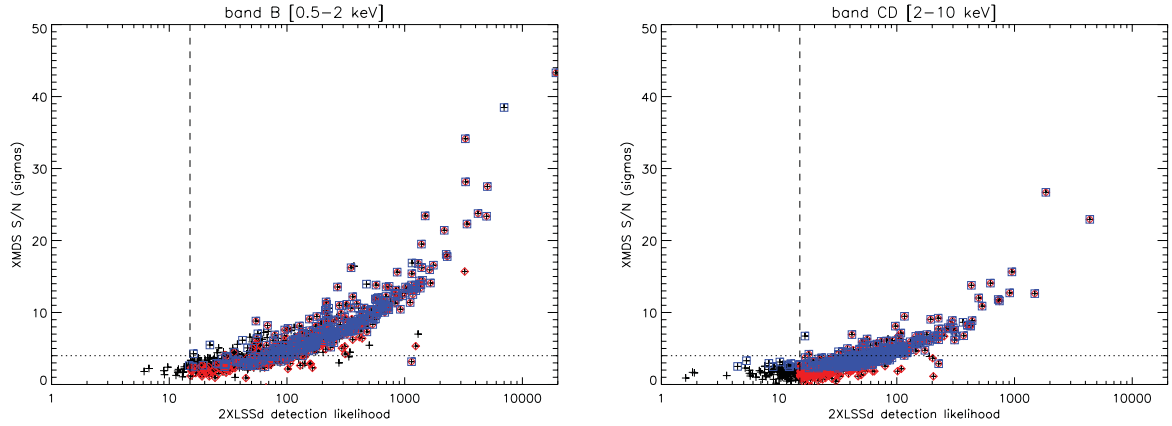

Figure C2. Cross-calibration between the 2XLSSd (XAMIN) detection likelihood and the XMDS signal-to-noise ratio: left, the soft band; right, the hard band. The dashed vertical line indicates the 2XLSSd acceptance thresholds of $LH > 15$, while the dotted horizontal line shows the conventional level of 4σ. Crosses indicate all objects detected in the given band. A (red) diamond surrounds the sources detected above LH threshold in both bands in 2XLSSd, while a (blue) square surrounds those detected above the chance probability threshold in both bands in the XMDS.

the 2XLSSd or 2XLSS catalogues might also involve adjacent B fields if the *XMM*–LSS overlap removal procedure preferred these. The association between XMDS and *XMM*–LSS sources is done within a radius of 10 arcsec. The comparison occurs naturally with the deep catalogue, because it involves the same input (ODF) event data (for the full exposures) with different pipelines and procedures. Of these 1168 objects, 1082 have a counterpart in the full exposure input tables, of which 1057 are catalogued in 2XLSSd, while 1019 have one in the 10-ks input tables, of which 956 are in 2XLSS.

Of the 86 XMDS sources not in the input table for 2XLSSd, we find the following.

23 are at off-axis angles greater than 13 arcmin (ignored by XAMIN).

39 are at large off-axis angles (>10 arcmin), so it is not surprising they were excluded by XAMIN.

Similarly, 43 are potential ultrasoft sources – the band with the highest signal-to-noise ratio in XMDS is the A band (0.3–0.5 keV), which is not processed by the current release of XAMIN – so they are legitimately excluded.

Considering the XMDS significance, 46 and 72 are below 3σ and 4σ, respectively.

If we allow the combination of different conditions, a net majority of the XMDS-only sources (76) are either ultrasoft, or at off-axis >10 arcmin or at $<3\sigma$.

We concentrate on the 1057 XMDS sources with a 2XLSSd correspondent (which can be called common catalogued). Of these, we find the following.

There are 783 in the same (G) field, so these should be exactly the same detections.

There are 173 stacked XMDS entries.

The remaining 103 cases associate sources detected in different pointings: 39 in another G field and 64 in a B field.

Concerning the distance between the (astrometrically corrected) X-ray positions in the XMDS and 2XLSSd catalogues, 58 per cent of the sources are closer than 2 arcsec, 88 per cent closer than 4 arcsec and only 4 per cent more distant than 6 arcsec, in general concentrated among the sources with lesser significance, and the few extended ones. The agreement between XMDS and 2XLSSd positions, peaking around 1 arcsec, is better than the typical inter-band distance between 2XLSSd detections in the two energy bands, which peaks around 2 arcsec. Compare Figs 5(c) and (d).

We have cross-calibrated graphically the detection likelihood of XAMIN with the chance probability of the XMDS (for definitions, see Baldi et al. 2002) and the detection likelihood of XAMIN with the significance in terms of number of σ of the XMDS (see Chiappetti et al. 2005, and references therein). We only show the latter in Fig. C2. We can see that a likelihood of 75 corresponds more or less to the 4σ level, and one of 40 to the 3σ level.

We also note that 89 per cent of the common sources have B as the best band (highest likelihood) in 2XLSSd. To be more precise, 96 per cent of the sources are observed by 2XLSSd in the B band, 62 per cent are observed in the CD band and 57 per cent are observed in both.

This can be compared with the totality of the 2XLSSd catalogue, where (with no appreciable difference between the full 2XLSSd catalogue and the sources in the G fields alone), 84 per cent of the sources have B as the best band, 89 per cent are observed in the B band, 48 per cent are observed in the CD band and 37 per cent are observed in both bands.

The XMDS, by construction, includes measurements in all five energy bands, even if the source is above the probability threshold only in one. If we consider as good detections for XMDS only those with $prob < 2 \times 10^{-4}$ in the band, of the sources in common with 2XLSSd, we find the following: 91 per cent are detected in the B band, 36 per cent in the CD band and 30 per cent in both.

The fluxes, computed for XMDS according to the prescriptions of Baldi et al. (2002) and for *XMM*–LSS, as explained in Section 3.1.1, are compared in Fig. C3. Extended sources classified as C1 are excluded because their 2XLSSd flux is set to undefined. The fluxes match qualitatively, although there is a systematic difference: 2XLSSd fluxes are 0.895 lower than the XMDS fluxes in the B band, while they are only 1.040 higher in the CD band.

It can be seen that a larger scatter in fluxes occurs for the sources which have poorer significance in either catalogue, while outliers are generally a result of sources presumably falling near a chip gap on one detector (and as such characterized by a

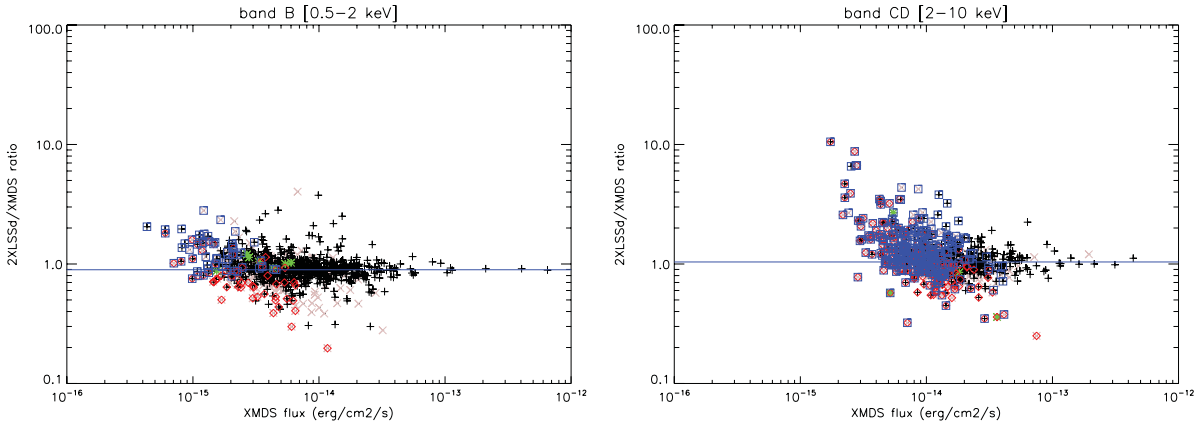

Figure C3. The ratio of the 2XLSSd and XMDS fluxes as a function of the XMDS flux for band B (left panel) and band CD (right panel). The horizontal solid line is a fiducial line corresponding to the actual average ratio in the band (see text). The (black) crosses indicate point-like sources which have a fluxflag of 0 or 1, the (pink) X those with a fluxflag of 2 (i.e. where the MOS and pn fluxes differ by more than 50 per cent). The (green) asterisks correspond to extended C2 sources for which the flux is computed from the point-like rates (C1 sources have flux set to undefined and are not plotted). A (red) diamond surrounds the points with a poor 2XLSSd likelihood $15 < LH < 20$ in the band. A (blue) square surrounds the points with a poor XMDS probability $prob > 2 \times 10^{-4}$ in the band. Note that the latter symbols are different from those used in Fig. C2.

fluxflag of 2), or exceptionally by residual C2 extended sources (for which the *XMM*–LSS flux is computed from the point-like rate).

C3.2 Comparison of the optical counterparts

It is also possible, similar to what was done in Section 5.2.2, to compare the counterparts in optical (and other) bands between the XMDS catalogue and one of our *XMM*–LSS catalogues. In doing this, we should consider the following.

(i) The identification procedure for XMDS is historically different from the one used here. In particular, it was carried out in several incremental steps, and it uses distances capped to 2 arcsec in the computation of probabilities.

(ii) The catalogues used for XMDS were in larger numbers (for a total of 27) and included many other, including older, data sources (e.g. VVDS, radio data, SIMBAD and NED, CFHTLS T003, etc.).

Therefore, we present a comparison limited to the 2XLSSOPTd catalogue (the one which matches XMDS better in exposures) and, for XMDS, to reduced counterpart sets considering only CFHTLS T004 D1 and W1, SWIRE DR6 and *GALEX*. UKIDSS was not included because 2XLSSOPTd uses release DR5plus, while XMDS uses release DR3. More specifically, we consider only the 1057 X-ray sources in common between XMDS and 2XLSSd, as described in Appendix C3.1.

These correspond to 4316 counterpart sets (of any rank) in 2XLSSOPTd and 4916 in XMDS. We find that a large fraction (3620) of the possible counterpart sets are identical (i.e. they have the same counterparts, irrespective of ranking, in both catalogues).

We can then concentrate on the best counterparts (ranks 0–1; a similar ranking system, though different in detail, was used also for XMDS), as follows.

For 627 cases (59 per cent of 1057), the best counterpart is exactly the same in all four D1, W1, SWIRE and *GALEX* catalogues, for 16 per cent in three catalogues (the other might be different or missing), for 15 per cent in two catalogues and for 4 per cent in one catalogue. This makes a total of 81 per cent with the choice of a highly compatible counterpart.

A very limited number of cases (five and eight) are potential blank fields in 2XLSSOPTd and XMDS, respectively, with another counterpart in the other catalogue.

The remaining 193 (18 per cent) cases select an altogether different counterpart in the two catalogues, as follows.

For 97 2XLSSOPTd and 77 XMDS sources, the counterpart set is present only in one catalogue and fully replaced by something else in the other.

In the other 96 or 116 cases, the counterpart set that is preferred in one catalogue is still present in the other with a different rank (secondary or rejected).

In conclusion, the compatibility between the counterparts is satisfactory.

C4 Comparison with 2XMM

We have briefly compared our 2XLSSd catalogue with the 2XMM catalogue (Watson et al. 2009). We have used the 2XMMi-DR3 'slim' reduced catalogue,[13] which contains exposure-merged sources (not individual detections) and therefore is immediately comparable). Thus, we compare with our post-overlap-removal catalogues.

We have restricted the comparison to a rectangular area fully encompassing 2XLSSd, and we note that such an area includes precisely just our pointings, with the only exception of a single additional pointing centred on the bright star Mira Ceti (ObsId 014850 0201).

The rectangular area contains 6181 2XMM sources. Because the slim catalogue does not contain indications on the pointings, we can tentatively flag sources in the Mira Ceti field as the 60 within 13 arcmin from the respective pointing centre. We have checked the association with our 6721 2XLSSd sources within the customary radius of 10 arcsec. We find that 5039 sources are associated, 1682 2XLSSd sources are not associated and 1141 2XMM sources are not associated.

[13] http://xmmssc-www.star.le.ac.uk/Catalogue/2XMMi-DR3cat_slim_v1.0.csv.gz

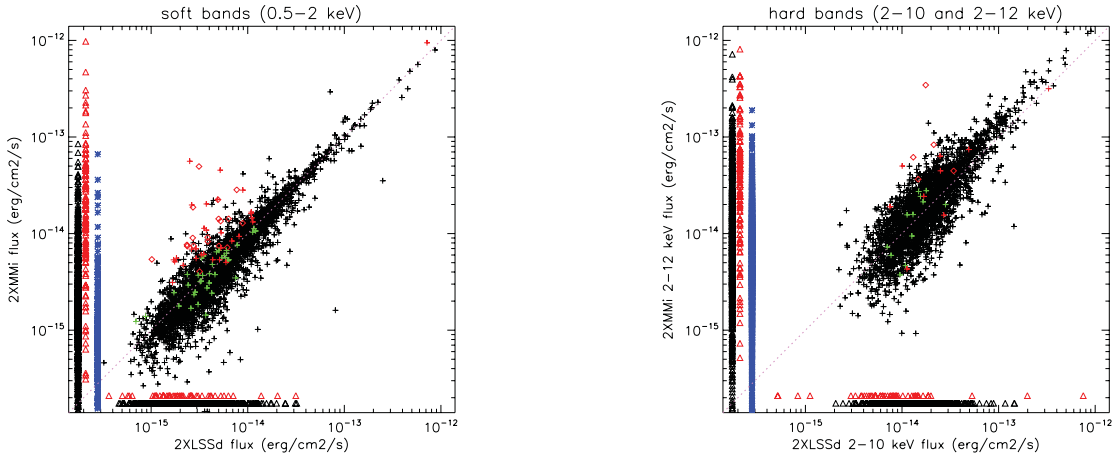

Figure C4. Comparison of the flux in the soft (left panel) and hard (right panel) energy bands. between 2XLSSd and 2XMM. Crosses and diamonds indicate point-like or extended objects associated in the two catalogues (see text). Blue asterisks indicate fluxes present but undefined in 2XLSSd, while triangles indicate sources present only in one catalogue (both are placed at a conventional out-of-range X or Y coordinate). Colour coding (only in the online version) is as follows: black crosses for point-like common sources, red diamonds for extended sources in both 2XLSSd and 2XMM, green crosses for 2XLSSd extended objects point-like in 2XMM; red crosses for 2XMM extended objects point-like in 2XLSSd; triangles are black or red for point-like or extended sources. Remember that fluxes for C1 extended sources are undefined in our data base (see table 9 in Paper I).

We note that 59 per cent of the unassociated 2XLSSd sources have a poor likelihood ($ML < 20$), and 93 per cent are below $ML < 40$ (i.e. 3σ). Despite the different definition of the 2XMM likelihood (parameter SC_DET_ML), we note that of the 1141 unassociated 2XMM sources, 67 per cent have SC_DET_ML < 15.

Of the associated cases, all but 69 have a single association. The ambiguous ones are all plain couples, and usually well separated (one 2XMM source at 1–2 arcsec from the 2XLSSd position, and the other at 8–9 arcsec).

The distance between the astrometrically corrected position (2XMM used the USNO catalogue for this purpose) for the associated primary (closest) cases is within 2 arcsec in 55 per cent of the cases, within 4 arcsec in 86 per cent of cases and within 6 arcsec in 95 per cent of cases (while 90 per cent of the 69 secondaries are above 6 arcsec). The histogram of distances peaks at a 1 arcsec offset (not unlike XMDS versus 2XLSSd).

The common subset contains 100 of our extended sources, and 88 2XMM extended sources (i.e. those with their parameter SC_EXTENT > 0). We find that 56 are considered extended in both catalogues, 110 of our extended sources do not appear at all in 2XMM, and 113 2XMM extended sources do not appear in 2XLSSd.

The 2XMM slim catalogue does not contain count rates. It contains fluxes in several energy bands, but these are different from ours. We can directly compare the sum of 2XMM bands 2 and 3 with our B band (0.5–2 keV), while at harder energies we can compare the sum of 2XMM bands 4 and 5 (2–12 keV) with our CD band (2–10 keV).

The comparison of the fluxes is reported in Fig. C4. The average 2XMM/2XLSSd flux ratio for common point-like sources is 0.92 in the soft band (same energy range) and 1.22 in the hard band (where 2XMM extends 2 keV further). Again, considering the differences in the pipelines, the agreement is acceptable.

This paper has been typeset from a TEX/LATEX file prepared by the author.